UNIVERSITY OF CALIFORNIA
RIVERSIDE

Utilization of PAH1 Disruptions for the Overexpression of Native P450s in *Yarrowia lipolytica*

A Thesis submitted in partial satisfaction
of the requirements for the degree of

Master of Science

in

Chemical and Environmental Engineering

by

Brandon Rayshawn Simmons-Rawls

December 2017

Thesis Committee:
Dr. Ian Wheeldon, Chairperson
Dr. Xin Ge
Dr. Yanran Li

The Thesis of Brandon Rayshawn Simmons-Rawls is approved:

_____

_____

_____

Committee Chairperson

University of California, Riverside

ACKNOWLEDGEMENTS

I would like to acknowledge the numerous people who have offered or given assistance through the journey in completing this degree. First and foremost I would like to thank my mom Valerie Rawls as without her love, support, and belief I would not have the courage to pursue this opportunity. Her ability to raise me by herself is an inspiration and a motivator to be able to be independent and capable. I would next like to thank my research group. The leader of the group, Dr. Ian Wheeldon, gave me the opportunity I sought to change my field and be able to grow effectively while in it. He was able to be encouraging and supportive during some of my lowest points while also dealing with my shortcomings and unfamiliarity with the material in the onset. I would like to thank Cory Schwartz for having the patience to train me and allow me to be inquisitive. I would like to acknowledge all of my current and previous lab mates: Aaron Toop, Aaron Lin, Priya Sengupta, Adithya Ramesh, Cody Jacobs, Ann-Kathrin Loebs, Samson Or, Yingning Gao, Lingling Zhu, Jan Schlemmer, Jordan Hall, Xuye Lang, Xiao Hong, Louis Lancaster, Sarah Thorwall, Keith Frogue, Jie Zhu, Ronja Engel, Mariajose Novelo, Megan Cook, and Josh Misa for their support during my stint in the lab. I would also like to thank Kimberly Claffey for helping provide me with the ability to support myself financially throughout the past two years through teaching chemistry and chemical engineering courses.

In addition I would also like to recognize the University of California, Riverside for providing a stimulating, engaging, and accepting atmosphere for its students. I would like to thank the Chemical and Environmental Engineering department for my admittance into the program. I would like to thank the faculty and staff within my department and all members of the Graduate Student Association in CEE with whom I've had the privilege of working. My gratitude is extended towards Dr. Xin Ge and Dr. Yanran Li for their guidance and willingness to take part in this journey. I would also like to say thank you to both Professor Alfred Center and Dr. James Pugh for their belief and recommendations for graduate school and the National Science Foundation Fellowship. I would like to thank the LGBT Resource Center at UCR for helping me become more comfortable with myself as well as provide a supportive community. Lastly, I would like to thank all of the friends I've made along the way who have helped in big ways and small to get me to this point.

DEDICATION

I dedicate this work to Valerie Rawls and Kevin Moye, both of whom I strive to improve myself for. I love you both very much.

ABSTRACT OF THE THESIS

Utilization of PAH1 Disruptions for the
Overexpression of Native P450s in *Yarrowia lipolytica*

by

Brandon Rayshawn Simmons-Rawls

Master of Science, Graduate Program in Chemical and Environmental Engineering
University of California, Riverside, December 2017
Dr. Ian Wheeldon, Chairperson

P450s have significant industrial relevance in the field of biotechnology and sustainability. In cells, they allow for the utilization of various substrates for energy usage and storage. Their ability to oxidize various substrates can also be beneficial to create anything from biofuel precursors to oleochemicals. As *Yarrowia lipolytica* produces a wide variety of P450s that catalyze disparate reactions, it presents itself as an ideal target for enzyme production. Genetic engineering methods for *Y. lipolytica* have made enzyme overexpression in the yeast more obtainable. This project aims to utilize genetic engineering tools available to *Y. lipolytica* in an attempt to overproduce P450s. Specific genes relating to protein expression will be targeted. This research hopes to prove the viability and capacity of *Y. lipolytica* as a large scale producer of membrane associated proteins by proliferating ER creation through altering carbon flux in the

organism. The experiments presented ascribe to quantify the potential of this microorganism with studies involving protein expression and cell morphology.

TABLE OF CONTENTS

CHAPTER 1 : INTRODUCTION 1

1.1 MOTIVATION 1

1.2 OVERVIEW OF LIPID SYNTHESIS AND STORAGE PATHWAY 4

1.3 OVERVIEW OF THE MONOOXYGENASE P450 ASSOCIATED WITH THE ALK2 GENE IN *YARROWIA LIPOLYTICA* 7

1.4 PREVIOUS WORK 9

1.5 OBJECTIVES 11

CHAPTER 2* CHAPTER 2: STUDYING THE CELLULAR EFFECTS OF PAH1 DISRUPTIONS IN *YARROWIA LIPOLYTICA 13

2.1 INTRODUCTION 13

2.2 METHODS AND MATERIALS 14

2.2.1 Strains, plasmids, and culturing 14

2.2.2 Growth curve analysis 15

2.2.3 Single Plasmid Transformation 15

2.2.4 Dual Plasmid Transformation 16

2.2.5 Genetic Engineering 16

2.2.6 Bodipy Staining 17

2.2.7 Fluorescent Imaging 17

2.2.8 Plate Reader Fluorescence 18

2.3 RESULTS AND DISCUSSION 18

2.3.1 PAH1 Disruption 18

2.3.2 Growth comparison 20

2.3.3 Lipid droplet comparison 22

2.3.4 ER Proliferation 28

2.3.5 Discussion 30

CHAPTER 3 CHAPTER 3: EXPLOITING PAH1 DISRUPTIONS FOR OVEREXPRESSION OF NATIVE ENZYMES 34

3.1 INTRODUCTION 34

3.2 METHODS AND MATERIALS 35

3.2.1 Strains, plasmids, and culturing 35

3.2.2 ALK2 Genomic Integrations 36

3.2.3 ALK2-GFP plasmid transformations 37

3.2.4 qPCR 37
3.2.5 SDS-PAGE 38
3.2.6 Western blot analysis 38
3.2.7 Flow Cytometry 39
3.2.8 Plate Reader Fluorescence 39
3.2.9 Fluorescent Imaging 39
3.3 RESULTS AND DISCUSSION 40
3.3.1 Genomic Integrations 40
3.3.2 Protein overexpression 42
3.3.3 Gene expression 45
3.3.4 ER capacity measurements 47
3.3.5 Discussion 50
CHAPTER 4 **CHAPTER 4: CONCLUSION & RECOMMENDATIONS** 53
CHAPTER 5 References 54

LIST OF FIGURES

Figure 1-1: Creation of anti-cancer drug Paclitaxel through the selective P450 oxidation of a biological precursor. The stereo-, regio-, and chemoselectivity of P450s is exemplified in the transition between taxa-4(5), 11(12)-diene and Baccatin III. 3
Figure 1-2: Lipid Synthesis pathways. Three pathways are included: Kennedy, Glycolysis, and CDP-Choline. Each contributes either directly or indirectly to the production of TAGs. G-3-P undergoes acylation to produce LPA. LPA is then acylated to PA. PA can either be dephosphorylated for the synthesis of DAG or CDP-DAG. CDP-DAG undergoes several enzymatic steps to create phosphatidylcholine (PC). PC can then be converted into DAG. DAG finally goes through a final acylation to generate TAG..... 5
Figure 1-3: Schematic representation of the P450 heme oxidation system. After oxidizing NADPH, electrons are transferred to the P450 heme where oxidation of the P450 substrate can take place. 8
Figure 2-1: Gene sequence of the target disruption site of pah1. The sequence in PO1f was targeted with a CRISPR/Cas9 system. The Δpah1 was reconstructed with incorrect non-homologous end joining adding a single adenine base..... 19
Figure 2-2: Partial translated protein sequence of PAH1. The protein sequence coincides with the region in the PAH1 gene disrupted with the CRISPR/Cas9 system. Bolded amino acids represent changes in translation due to codon changes. The strain with disrupted PAH1 has a stop codon represented by an asterisk..... 19
Figure 2-3: Growth curve analysis of PO1f and Δpah1 Y. lipolytica stains. Cell were grown in (A) YPD and (B) YTO media..... 21
Figure 2-4: Fluorescent images of LDs in Y. lipolytica. Images were taken at 32 hours from nitrogen-limited media for optimal LD production. ERG6-DS Red localizes to the outside of the LDs while Bodipy stains the entirety of the LD. Overlay of images revealed that there is consistent localization of Bodipy to the LDs..... 24
Figure 2-5: Sample cell field of Bodipy 493/503 staining. These cells were grown in nitrogen-limited media to induce LD formation. Cell membranes are shown in blue and LDs in green..... 25
Figure 2-6: Sample LD field processed in ImageJ. The brightness threshold of the cell images were increased to over 150. Images were converted to black and white for better analysis..... 26
Figure 2-7: ImageJ LD recognition and counting. Black and white LD fields were analyzed in ImageJ software with a 25 square pixel minimum size exclusion parameter and a 0.25 circularity parameter..... 26
Figure 2-8: LD size distribution of PO1f and engineered strains. Cells were grown in nitrogen-limited media to stationary phase at 24 hours 28
Figure 2-9: Fluorescent imaging of Alk2-GFP in PO1f and Δpah1. Images were taken of (A) PO1f background and (B) Δpah1 background with a FITC filter set..... 29
Figure 2-10: Plate reader fluorescence of yeast strains. Strains were transformed with ALK2-GFP and measured with an 485 nm excitation and 508 nm emission wavelength 30
Figure 3-1: Three primer amplification system for determination of ALK2-V5 integrations into Y. lipolytica genome. Primers flank homology regions. 41

Figure 3-2: Gel electrophoresis of amplified genomic fragments from the three primer system. The sample used a 1 kb ladder with three possible results in each sample lane: 1 kb, 2 kb, and both bands. 41
Figure 3-3: Western blot analysis and SDS-PAGE of Y. lipolytica samples. Each additional ALK2-V5 integration is represented by designation 1, 2, or 3. Each lane is a corresponding SDS sample and Western signal. 44
Figure 3-4: Western intensity comparisons. Western samples were normalized to PO1f with a single ALK2-V5 integration. 45
Figure 3-5: Average qPCR copy number fold change of each strain relative to PO1f background. Samples were grown to mid-stationary phase in rich media. 46
Figure 3-6: Comparison of relative gene expression versus protein expression for ALK2 genes 47
Figure 3-7: Fluorescent imaging of stains transformed with ALK2-GFP. Each set of images represent the following number of integrations of ALK2-V5: (A) 0, (B) 1, (C) 2, and (D) 3. 49

LIST OF TABLES

Table 2-1: Yeast strains and plasmids used in Chapter 2 experiments 14
Table 2-2: Yarrowia lipolytica strains 22
Table 3-1: Yeast strains and plasmids used in Chapter 3 experiments 35
Table 3-2: Integration efficiency of ALK2-V5 cascade into subsequent sites. 42

CHAPTER 1 : INTRODUCTION

1.1 MOTIVATION

Microorganisms are a robust set of fast growing organisms that are considerably simpler than their larger, multi-celled eukaryotic counterparts. In the biotechnology field this simplicity serves as a benefit thanks to the ease of elucidating different aspects of the genome and the interplay of genes. Furthermore, gene editing tends to be easier as there are less chromosomal sets and thus a smaller probability of large replicate gene sequences. This coupled with the quick growth of cells means that the alteration of these organisms for industrial or academic utilization has a short turnaround time.

It is for these reasons that many microorganisms have been studied for their use for different industrial applications. One of the first such studies centered on the antibiotic penicillin. This was produced in the *penicillium* strain of fungi. Now species such as *Saccharomyces cerevisiae*, also known as baker's yeast, are used as model yeasts utilized for the production of many pharmaceuticals and other commodity chemicals (Gao, et al., 2016). One application of particular interest is lipid production for the generation of specialty chemicals (Friedlander, et al., 2016). Oleaginous yeasts such as *Yarrowia lipolytica*, the organism used in this study, have an advantage in lipid production as they naturally generate and store lipids at high levels due to complex internal membranes (Qiao, Wasylenko, Zhou, Xu, & Stephanopoulos, 2017). Metabolic engineering and adaptive evolution have been utilized to further push lipid production in this microorganism to roughly 90% of its biomass (Li & Alper, 2016). Through the metabolic engineering for increased lipid production in *Y. lipolytica* and other organisms

however, other potential applications have been discovered, including the expression of P450s which is the main goal of this study.

Beyond the ability of yeast to produce lipids, there is also substantial interest in expressing proteins and metabolites. One in particular is the set of hemoproteins referred to as P450s. They are conserved across various species in a wide range of kingdoms (Iwama, et al., 2016). In yeasts they are commonly known for their ability to oxidize substrates to be used for growth (Scheller, Zimmer, Becher, Schauer, & Schunck, 1998). The products of this oxidation however can also be beneficial for anything from pharmaceuticals to biofuels. For instance, saponins, a diverse family of triterpenes, have several steps within its production catalyzed by P450s (Arendt, et al., 2017). Saponins exhibit pharmacological properties along with their respective aglycones and sapogenin (Arendt, et al., 2017). Another example of utilization of P450s, as shown in Figure 1-1, is the diterpenoid paclitaxel, a well-known cancer drug. The regio-, chemo-, and stereoselective oxidation helps convert a precursor molecule taxa-4(5), 11(12)-diene into the final product (Kaspera & Croteau, 2006).

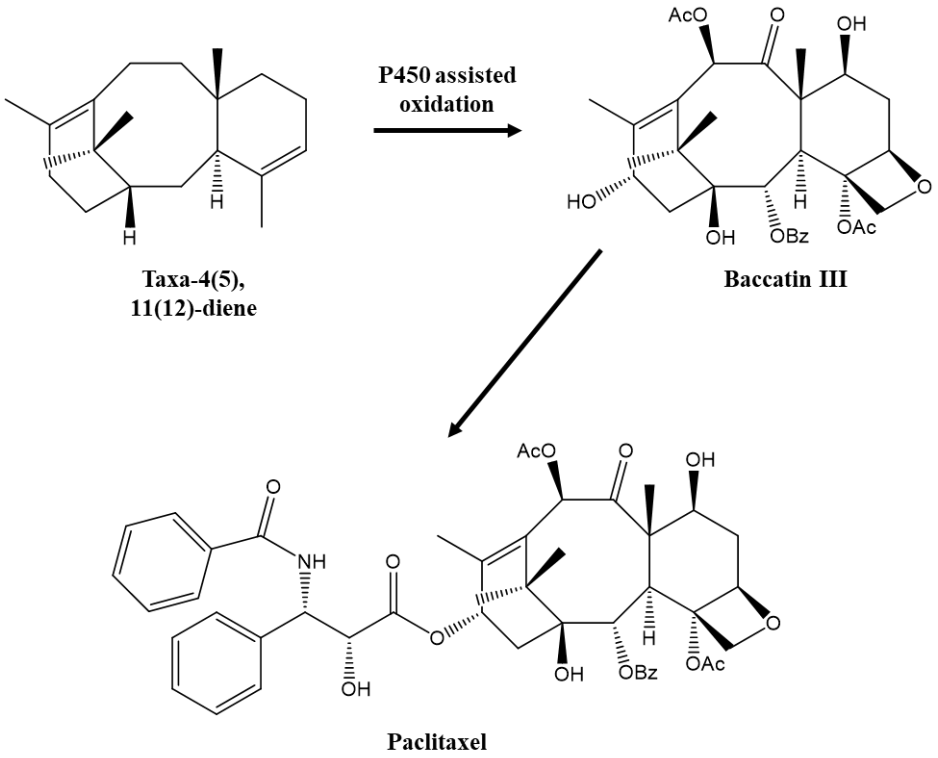

Figure 1-1: Creation of anti-cancer drug Paclitaxel through the selective P450 oxidation of a biological precursor. The stereo-, regio-, and chemoselectivity of P450s is exemplified in the transition between taxa-4(5), 11(12)-diene and Baccatin III.

Yarrowia lipolytica represents the potential of lipid accumulating organisms. As stated previously the lipids can be used for industrial purposes; however, if the ability for it to do so stems from membranes, such as the ER, studying ER physiology and utilizing it to compartmentalize specific cellular actions could prove beneficial in industrializing this yeast strain. Of more interest is the potential for homologous expression of industrially relevant enzymes like the previously mentioned P450s. *Y. lipolytica* has been shown to have high heterologous expression of several stable, active proteins coupled with high transformation frequency within the strain of yeast (Muller, Sandal, Kamp-Hansen, & Dalboge, 1998). The purpose of this study is therefore to determine the effects

of changing physiology of the ER in *Yarrowia lipolytica* and to determine the change's potential to be useful in utilizing or producing cellular components like membrane associated enzymes in greater quantities.

1.2 OVERVIEW OF LIPID SYNTHESIS AND STORAGE PATHWAY

Fatty acids and dicarboxylic acids represent lucrative compounds to be used for industrial applications (Notonier, Gricman, Pleiss, & Hauer, 2016). Their incorporation into lipids means that they can aid in the production of oleochemicals like surfactants, lubricants and pharmaceutical products (Souza, Ramos, Schwan, & Dias, 2016). In addition, fatty acids are utilized in the creation of biofuels, which are alternatives to petroleum-based fuels with similar energy content (Sheng & Feng, 2015). Oleaginous microorganisms, like *Y. lipolytica*, have a comparative advantage in endeavors to create fatty acids as they can naturally accumulate lipids to quantities comprising up to 20% (wt./wt.) of their dry cell weight (Souza, Ramos, Schwan, & Dias, 2016). Genetic engineering has proven this accumulation can be pushed to up to 90% (wt./wt.) of the dry cell weight, furthering this organism's industrial potential.

Lipids within cells are generally stored as neutral lipids within organelles called lipid droplets (LDs) (Beopoulos, et al., 2008). These droplets are comprised of triacylglycerols (TAGs) and sterol esters (SEs) which are primarily produced through the Kennedy pathway (Beopoulos, et al., 2008). The Kennedy pathway, as shown in Figure 1-2, takes a dihydroxyacetone phosphate (DHAP) intermediate from the glycolysis pathway and converts it to either a TAG or SE by utilizing fatty acids, acyl-CoA, and a plethora of catalytic enzymes. Out of these two compounds, TAGs are seen as more

interesting for their inclusion of three fatty acids and their more complex pathway to creation.

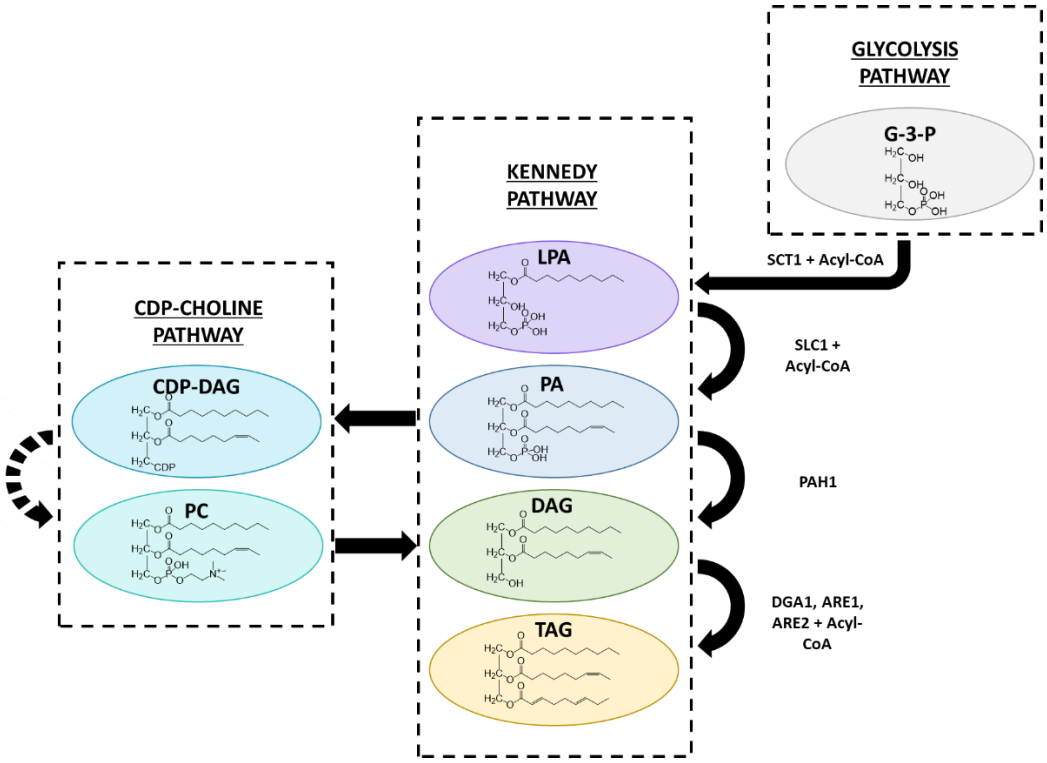

Figure 1-2: Lipid Synthesis pathways. Three pathways are included: Kennedy, Glycolysis, and CDP-Choline. Each contributes either directly or indirectly to the production of TAGs. G-3-P undergoes acylation to produce LPA. LPA is then acylated to PA. PA can either be dephosphorylated for the synthesis of DAG or CDP-DAG. CDP-DAG undergoes several enzymatic steps to create phosphatidylcholine (PC). PC can then be converted into DAG. DAG finally goes through a final acylation to generate TAG.

In order to generate TAGs, one of two paths is taken. The first path utilizes the CDP-choline pathway, an area of the Kennedy pathway, to create diacylglycerols (DAGs). These DAGs can then either use an acyl-CoA dependent path using a DAG acyltransferase or an acyl-CoA independent path with glycerophospholipids and phospholipid DAG acyltransferase to form TAGs (Beopoulos, et al., 2008). The second path begins with the dihydroacetone phosphate (DHAP) from the glycolysis pathway.

DHAP is first hydrogenated to give the starting glycerol-3-phosphate (G-3-P) component needed for the path. G-3-P is converted to lysophosphatidic acid (LPA) via acylation, then to phosphatidic acid (PA) via a secondary acylation, and finally to DAG after dephosphorylation. These DAGs are then converted to TAGs with the acyl-CoA dependent and independent paths mentioned earlier.

As the Kennedy pathway is the primary metabolic pathway for the synthesis, storage, and degradation of TAGs and other lipids, the pathway invites the interest of targeted research for studying FAs and lipids. In particular, there is interest in modifying lipid composition and fatty acid prevalence as it can provide avenues to generate viable chemicals intracellularly. Longer chain hydrocarbons are one of these chemicals. Traditionally, they are generated through processing petroleum (Souza, Ramos, Schwan, & Dias, 2016). However, some microorganisms have shown the capacity to create similar length hydrocarbons in different forms (Souza, Ramos, Schwan, & Dias, 2016). This means that metabolites from the Kennedy pathway may be able to be used to alternatively derive products such as oleochemicals and biofuel precursors without the use of petroleum, therefore generating a sustainable model.

Because of the potential for generating biofuel precursors and other components through lipid biosynthesis, manipulations of the Kennedy pathway have been done in other studies. One prominent manipulation is of the phosphatidic acid dephosphorylase coded by the gene PAH1. Changes in the activity in this gene have resulted in physiological changes in cells. For yeasts, disruptions in the PAH1 gene have resulted in drastic decreases in LD number and even complete absence of LDs once steryl

acyltransferases lose activity (Adeyo, et al., 2011). In *S. cerevisiae* changes in PAH1 directly correlate to the accumulation of PA in the cells (Carman & Han, 2009). This is turn affects the regulation of phospholipid synthesis gene expression (Carman & Han, 2009). The change in regulation of phospholipid synthesis gene expression is part of the interest in this study. Increasing this gene expression subsequently increases phospholipid presence in the cells. Higher quantities of phospholipids have been shown to lead to greater expression of native membrane proteins within our strain of interest *Y. lipolytica* (Guerfal, et al., 2013). It is our hope to capitalize on this by facilitating greater protein quantities through genetic manipulation. The target protein of this study is the ALK2 associated P450 of *Y. lipolytica*.

1.3 OVERVIEW OF THE MONOOXYGENASE P450 ASSOCIATED WITH THE ALK2 GENE IN *YARROWIA LIPOLYTICA*

Monooxygenases (MOs) are considered commercially interesting enzymes. MOs include various catalysts that have the ability to oxidize a variety of substrates at different functional positions. For instance MOs can have the ability to oxidize anything from methane and ethane to hexadecane (Bordeaux, Galarneau, & Drone, 2012). In other cases MOs can be involved in drug metabolism (Nebert & Russell, 2002), oxidizing plant metabolites, and activating carcinogenic compounds (Shimada & Fujii-Kuriyama, 2003). This activity is also commonly used by cells to convert certain substrates into fuel that is often utilized by cells immediately for growth or stored for later usage. However, the creation of chemicals such as fatty alcohols through oxidation via MOs, and the subsequent conversion into fatty acids with other enzymes, provides the framework for the production of numerous oleochemicals for industrial use. MOs not only contain the

ability to begin the process of FA generation, but some include the reactivity with FAs to inevitably create dicarboxylic acids.

One specific monooxygenase is the conserved family of enzymes known as P450s. P450s are most commonly known for the oxidation at C-H (sp^3), C-H (sp^2), C-C double bonds, and heteroatoms (Fasan, 2012). This oxidation is done through a dual component system consisting of the heme P450 and the reductase (Fasan, 2012). The reductase can either be flavin adenine dinucleotide (FAD) or flavin mononucleotide (FMN). The reductase reduces NADPH to $NADP^+$ retrieving electrons from the compound. The electrons are then shuttled to the heme P450 which uses the electrons to reduce oxygen. The reduced oxygen is then electrophilic and can be added to the substrate. The basic schematic of the P450 system is shown in Figure 1-3.

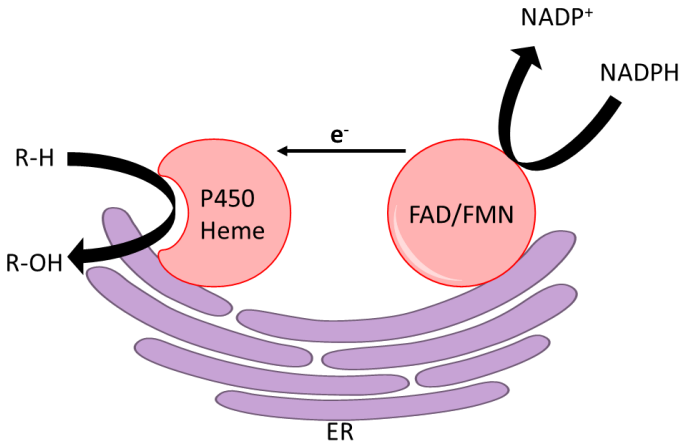

Figure 1-3: Schematic representation of the P450 heme oxidation system. After oxidizing NADPH, electrons are transferred to the P450 heme where oxidation of the P450 substrate can take place.

Yarrowia lipolytica, like many organisms, have native, membrane-bound, P450s coded in its genome. For *lipolytica* this includes a set of ALK genes from 1-12 (Iwama, et

al., 2016). Each of these ALK-associated P450s utilize different substrates including long chain fatty acids or alkanes (Iwama, et al., 2016). This activity is of interest to the previously stated objectives of creating metabolites that are industrially viable.

Utilizing these native P450s have several benefits. *Y. lipolytica* for one has an unfolded protein response that can easily orient native proteins into their correct configuration (Guerfal, et al., 2013). Also, it potentially allows for the ability to compartmentalize large scale fatty acid and dicarboxylic acid production with genetic manipulation (Fickers, et al., 2005). Furthermore, in comparison to other yeasts including *Klyveromyces lactis, Pichia pastoris,* and *Schizosaccharomyces pombe, Y. lipolytica* has been shown to secrete more active protein, of order of magnitude difference, in relation to its cell count while still maintaining a high transformation frequency (Muller, Sandal, Kamp-Hansen, & Dalboge, 1998). P450s association to the ER means that the ER's proliferation can lead to excess P450s, which can be further maximized by using *Y. lipolytica* as the organism to harbor expression.

1.4 PREVIOUS WORK

Studies of P450s in *Y. lipolytica* are fairly recent. There have been experiments done to heterologously express each of the previously stated ALK genes of *Y. lipolytica* into model yeasts like *S. cerevisiae* and bacteria like *E. Coli* (Iwama, et al., 2016). This aided in the elucidation of substrate specificity of each particular protein. However, *in vitro* expression has the shortcoming of removing natural responses to the P450s in the host organism (Guerfal, et al., 2013). While substrate specificity is important, *in vitro* expression does not reveal physiological effects of the P450s on the cell. It also does not

provide evidence of various molecular functions or interplay relations with native genes (Guerfal, et al., 2013). This information is important as homologous expression produces more stable products than heterologous expression. Therefore, it is ideal to express the P450s in their native system.

Though *in vivo* expression is preferred for the production of stable P450s, research has been stymied due to the relatively low abundance of these native proteins (Guerfal, et al., 2013). This is compounded with the difficulty of purifying stable membrane proteins in sufficient quantities (Guerfal, et al., 2013). Ascertaining P450 structure in *Y. lipolytica* has thus been hindered. It is therefore of interest to discover methods to natively express these P450s in greater quantities.

As recombinant gene expression has been ruled out for its lack of revealing host cell effects, altering cell physiology has been utilized as another avenue of protein expression increase (Guerfal, et al., 2013). Previously, it was hypothesized that ER proliferation in cells has the potential to bolster the presence of membrane-bound proteins like P450s (Guerfal, et al., 2013). One method done to proliferate the ER was the disruption of the phosphatidic acid dephosphorylase coding gene PAH1 (Arendt, et al., 2017). In both *Saccharomyces* and *Y. lipolytica* ER proliferation was observed visually, but not quantified (Arendt, et al., 2017). Increased membrane protein was also documented (Guerfal, et al., 2013). This makes targeting ER proliferation through PAH1 disruption a potentially viable solution for P450 overexpression.

One drawback to PAH1 disruption however has been lack of quantifying evidence. Work has been performed to show proliferated ER after PAH1 deletion through

transmission electron microscopy (TEM) (Arendt, et al., 2017). This method does not, however, reveal the relative change of ER levels from a wild type background. It is thus tenuous to say overexpressions from this gene edit would produce concentrations high enough for characterization or industrial utilization. Furthermore, low expression levels obstruct discerning whether the overexpression P450s are active (Guerfal, et al., 2013). To rectify this, my study includes engineered overexpressions into *Y. lipolytica* through CRISPR/Cas9 designed insertion vectors. This overexpression should lead to protein levels high enough for use in characterization.

1.5 OBJECTIVES

P450s have widespread commercial appeal to oleochemical and biofuel industries. PAH1 has been seen as an attractive target for modifying the production of P450s in microorganisms to increase its availability to markets. The objective of this thesis is to study the cellular effects of altering carbon flux of the Kennedy pathway via a disruption in PAH1. More importantly the aim is to determine whether the anticipated effects of this genetic modification can be advantageous to endeavors involving membrane protein overexpression. To elucidate the potential advantages, this work investigates the change in protein levels and the functionality associated with the varying levels.

Chapter 1, this chapter, introduces the scientific interests of P450 production and PAH1 disruption in *Y. lipolytica*. A brief overview of the pathways that would be affected by changes to PAH1 are discussed, as well as the hypothesized effects these alterations would have on the cell morphology. In addition the catalytic properties of P450s in *Y. lipolytica* are discussed. Finally, the objective of each chapter of this thesis is detailed.

Chapter 2 details the quantification of the phenotypic changes associated with deletions in the phosphatidic acid dephosphorylase coding gene PAH1. ImageJ analysis software was utilized to determine any variations in LD sizes. Flow cytometry and plate fluorescence experiments were used to differentiate ER proliferation within cell populations.

Chapter 3 provides the analysis of P450 overexpression in engineered strains. Quantitative PCR is used to determine the gene expression associated with the genomic integration of ALK2 cassettes. Western blot analysis was utilized to determine relative protein expression and fluorescent imaging was performed to compare limitations in ER capacity. Lastly, carbon monoxide assays were conducted to determine activity changes between wild type and engineered strains.

Finally, the studies in chapters 1-3 are summarized and suggestions for future work are discussed in chapter 4.

CHAPTER 2 : STUDYING THE CELLULAR EFFECTS OF PAH1 DISRUPTIONS IN *YARROWIA LIPOLYTICA*

2.1 INTRODUCTION

PAH1 is a gene that codes for a phosphatidic acid dephosphorylase enzyme (PAP) in *Yarrowia lipolytica* and other organisms (Carman & Han, 2009). This enzyme is responsible for dephosphorylating PA into DAG. Therefore, mutations in this gene can cause the PAP not to be translated properly, thus rendering the PAP inactive. This can lead to several defects, as it does in *Saccharomyces cerevisiae*, including growth defects, fatty acid-induced lipotoxicity, and TAG reduction (Guerfal, et al., 2013). Furthermore, it has the potential to alter the prevalence of PA in the cell.

Due to PAs utilization in multiple pathways, predominantly the Kennedy and CDP-Choline pathways, the cellular effects in *Y. lipolytica* stemming from PAH1 disruptions have previously been hypothesized. Theories developed stating that this genome edit would affect two organelles in particular: the endoplasmic reticulum and lipid droplets (Xu, Su, & Carman, 2012). The former would be proliferated as the excess PA in the CDP-Choline pathway would generate more phospholipids to be incorporated into membrane organelles like the ER (Han, O'Hara, Carman, & Siniossoglou, 2008). The latter would be reduced as one of the main components, TAGs, would be hindered in its production (Guerfal, et al., 2013). Although TEM has been a method to differentiate changes in cell physiology from a PAP disruption, this provides only qualitative data.

The goal of this chapter is to provide quantitative evidence of the changes between PO1f and *Δpah1* strains of *Y. lipolytica*. To achieve this, the growth

characteristics, ER proliferation, and LD size and number will be compared to glean whether there are exploitable variations between strains

2.2 METHODS AND MATERIALS

2.2.1 Strains, plasmids, and culturing

Plasmids and strains utilized in this studied are listed in Table 2-1. All strains used in this study were engineered from the YS363 PO1f strain of *Y. lipolytica*. Yeast cultures that were used for transformation were grown in YPD (2% glucose, 2% peptone, and 1% yeast extract). Yeast used for studies involving lipid comparison (nitrogen starvation conditions) were grown in YNB (2% glucose, 1% yeast extract, 1.7g/liter yeast nitrogen base without amino acids). Yeast transformed with overexpression plasmids were grown in synthetic dropout media, SD (2% glucose, 0.69 g/L CSM-Leu, 1.7 g/L nitrogen base w/o amino acids). Unless otherwise stated all samples were taken from their respective cultures at 24 hours during the stationary phase of growth.

Table 2-1: Yeast strains and plasmids used in Chapter 2 experiments

Strain	Genotype/Description	Marker
Yarrowia lipolytica		
YS394	YS363 + pIW223	Amp/LEU
YS952	YS363 + pIW225	Amp/LEU
YS953	YS621 + pIW225	Amp/LEU
Plasmids	**Genotype/Description**	
pIW 223	TEF-ERG6-DSRed-CYC1	Amp/LEU
pIW 225	TEF-ALK2-GFP-CYC1	Amp/LEU
pIW 505	TEF-Cas9-CYC1-5' GCTCTGAACGACTCTAAACA3'sgRNA	Amp/LEU

2.2.2 Growth curve analysis

Yeast strains were grown overnight in either rich YPD media or synthetic dropout media with the appropriate auxotrophic dropout supplement. Cells were then normalized by OD and inoculated into 25 μL of media in a baffled flask. The flasks were shaken at 220 RPM and at 28ºC with the OD measured roughly every hour with a Thermo Scientific Nanodrop 2000c spectrophotometer. Each strain was done in triplicate and the results averaged with error included.

2.2.3 Single Plasmid Transformation

Single plasmid transformation was performed with a Frozen-EZ Yeast Transformation kit purchased from Zymo Research. This kit utilized a lithium acetate based transformation protocol. Yeast strains were grown overnight and then inoculated in a 1:10 ratio in the appropriate rich or minimal media. After the strains reached exponential phase, 4-6 hours after inoculation, the cells were pelleted and resuspended in EZ1 solution. Cells were again pelleted and suspended in EZ2 solution. Approximately 1 μg of DNA was introduced to 50 μL of the competent cells. An additional 500 μL of EZ3 was added to the competent cells and the solution incubated for 45 minutes. The cells were also vortexed every 15 minutes of the inoculation. Samples were either plated or inoculated in liquid media for 2-4 days. Strains with fluorescent markers were imaged to ensure proper transformation. Strains intended to alter genomic code were subjected to colony PCR. The amplicon was then sent for Sanger sequencing to check the for the appropriate genome edits.

2.2.4 Dual Plasmid Transformation

Strains were grown to overnight to stationary phase and 250 μL were pelleted. The supernatant was discarded and the pellet washed with 250 μL of transformation buffer (0.3M lithium acetate, 10mM Tris-HCl, 1mM EDTA). Cells were pelleted and resuspended in 100 μL of transformation buffer. Then the following components were added in order and mixed via pipetting: 3 μL SS DNA mix (8 mg/mL salmon sperm DNA, 10mM Tris HCl, 1mM EDTA), 1 μg of plasmid DNA, and 15 μL BME mix (95% vol./vol. Triacetin, 5% vol./vol. BME). Cells were then incubated for 30 minutes at room temperature and 70 wt% PEG was added and mixed via pipetting. The cells were again incubated for 30 minutes at room temperature and then heat shocked for 15 minutes at 37ºC. The cell suspension had 1 mL of H_2O added, was spun down, and introduced to the appropriate selective media for outgrowth over 2-4 days. For strains intended to have genomic alterations, colony PCR was performed to ascertain the existence of integrations. Amplicons were sent for sequencing with positive samples being grown in YPD to induce selective pressure removal of the plasmids.

2.2.5 Genetic Engineering

Genomic editing was done using a CRISPR/Cas9 editing system on plasmid DNA. The plasmid has two markers for selection. AmpR allows the plasmid to be amplified in competent *E. Coli* cells after proper cloning. Leu2 promotes growth of transformed strains minimal media.

The CRISPR/Cas9 plasmid included a 20 base pair PAM sequence, a sequence preceding a NGG segment, that was followed by sgRNA which targeted the PAM

sequence in the genome. The Cas9 protein then induced a double stranded break in the genomic DNA.

Repairs in the genome were done with either homologous recombination (HR) or non-homologous end joining (NHEJ). When the genome was repaired with NHEJ there were instances of single base deletions or the addition of an adenine (A) base. This constituted a disruption that lead to *Δpah1* background strains.

2.2.6 Bodipy Staining

The Bodipy staining solution was created with 100 µg of Bodipy 493/503 per µL of ethanol. Cells were washed twice with 1 mL of phosphate buffer solution (PBS). They were then resuspended in 1 mL of PBS and 10 µL of Bodipy solution introduced. The cell solution was then covered and put on ice for 10 minutes before being used for fluorescent imaging.

2.2.7 Fluorescent Imaging

Imaging was done with an Olympus BX51 fluorescent microscope at the time point specified for the experiment. Samples were washed twice in PBS before being prepared on glass slides for visualization. Bright light images were taken for the full images of the cell membrane and other organelles discernible without stains. Strains transformed with DS Red fluorescing plasmids were imaged with a Texas Red filter set. Samples stained with Bodipy 493/503 were imaged with a FITC filter set. All images were recorded with a QImaging Retiga Exi Fast 1394 camera in cellSens Dimension software. Images were processed via deconvolution and all bright fields were combined with respective fluorescent views.

Processed images were subjected to analysis in ImageJ software. Threshold color was set to black & white and brightness set to above 150, eliminating the cell membranes. The image was then set to binary and as to apply Watershed and Fill Holes commands. Watershed separated any entities with overlap that were considered LDs. Fill Holes completed objects that had variable fluorescence within its perimeter. Analyze Particles was then selected to present a dataset of LD sizes. The minimum size was set to 25 square pixels to eliminate insignificant fluorescent signals. Circularity minimum was set to 0.25 to filter out erroneous fluorescent marks or residual membrane fluorescence. Resulting area measurements were then used for LD comparison.

2.2.8 Plate Reader Fluorescence

Strain samples were grown in triplicate to stationary phase and normalized based on OD. Cell were then washed twice with water and suspended in 200 µL of water. Samples were loaded into a black CorningStar 96-well plate and fluorescence measured with a 485nm excitation and 508nm emission filter. The sensitivity setting was set to 100 due to promoter strength.

2.3 RESULTS AND DISCUSSION

2.3.1 PAH1 Disruption

In order to determine the effects of PAH1 on *Y. lipolytica*, the native gene was targeted for disruption. To find the native PAH1 gene, the pah1p homologue in *S. cerevisiae* was found using a *Saccharomyces* genome database. The protein sequence was then subjected to the sequence matching tool BLAST in NCBI against all chromosomal

sets in the *Y. lipolytica* strain PO1f. The gene sequence of the protein that most closely matched the pah1p from *Saccharomyces* was determined to be the PAH1 gene.

The disruption was achieved with the utilization of a CRISPR/Cas9 genetic editing tool. The system was developed on a singular plasmid with the sgRNA programmed to target a 20 base pair sequence within the PAH1 gene that preceded an appropriate PAM sequence (NGG) and was not an intron. Disruptions were achieved when native enzymes responsible for non-homologous end joining incorrectly reassembled the double stranded break induced by the CRISPR/Cas9 system. To check for gene disruptions, the target disruption site of PAH1 was flanked with two primers and amplified. The amplified fragments were then sequenced and compared with the sequence from the wild type strain. The resulting misalignment, as seen in Figure 2-1, caused a genetic shift, presumably creating a different translated protein.

```
PO1f pah1:   TGAGCCGGACTACCTTGCTCTGAACGACTCTAAA–CAGGGTGGCGA
Δpah1 :      TGAGCCGGACTACCTTGCTCTGAACGACTCTAAAACAGGGTGGCGA
```

Figure 2-1: Gene sequence of the target disruption site of pah1. The sequence in PO1f was targeted with a CRISPR/Cas9 system. The *Δpah1* was reconstructed with incorrect non-homologous end joining adding a single adenine base.

The single base addition that was achieved from genome editing was checked to ensure changes were observed within the translated protein. The protein translations are shown in Figure 2-2 below.

PO1f pah1: PSSSPSWGQEEGGDGEPDYLALNDSK**QGGDSKHGRSPSEGPPFRSPSADHL**
Δpah1: PSSSPSWGQEEGGDGEPDYLALNDSK**TGWRQQARQIALGGPTIQITFGGSLT***

Figure 2-2: Partial translated protein sequence of PAH1. The protein sequence coincides with the region in the PAH1 gene disrupted with the CRISPR/Cas9 system. Bolded amino acids represent changes in translation due to codon changes. The strain with disrupted PAH1 has a stop codon represented by an asterisk.

The original pah1p from *Y. lipolytica* had a size of 79.3 kDa with 723 amino acids translated. The disruption caused the protein sequence to be altered as well as shortened. The newly translated protein is 8.7 kDa with 82 amino acids. This drastic reduction in protein size and the substantial change in protein sequence suggest the PAP encoded by PAH1 has lost its activity.

2.3.2 Growth comparison

The PO1f and the PAH1 disrupted strain were subjected to growth analysis to determine if there would be discernible differences in growth stemming from the inactivity of PAP. As it had been previously hypothesized that the uptake of oleic acid as a carbon source would be stunted in the PAH1 disrupted strains, both PO1f and *Δpah1* were subjected to growth analysis in YTO (oleic acid) media. Strains were also grown in YPD (rich media) to act as a control for the YTO growth experiments.

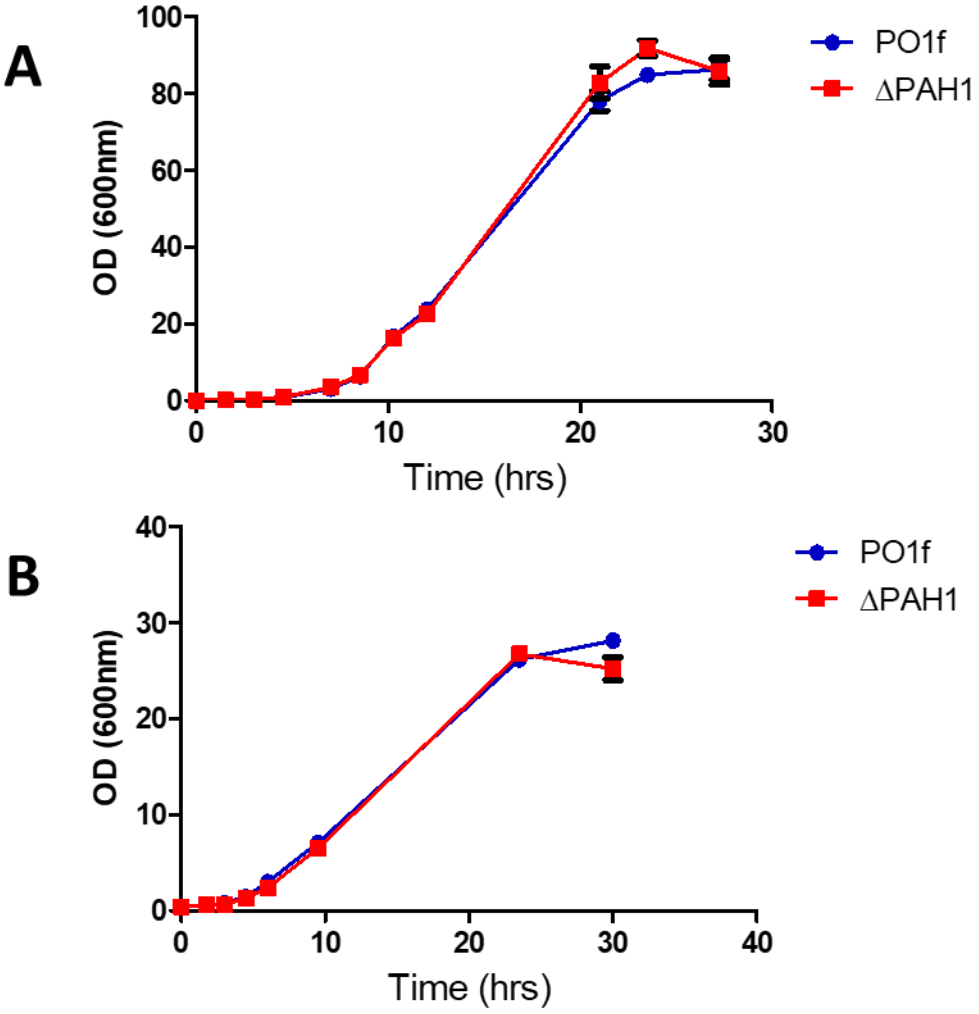

Figure 2-3: Growth curve analysis of PO1f and *Δpah1 Y. lipolytica* stains. Cell were grown in (A) YPD and (B) YTO media

It was previously expected that *Δpah1* would have a longer lag phase in YTO media due to an induced inhibition to uptake oleic acid but uninhibited growth in YPD (Guerfal, et al., 2013). However, the growth of both tested strains were roughly the same for both growth mediums with no significant delay of the exponential phase in YTO as seen in Figure 2-3. The difference from the expected extension of the lag phase after the

PAH1 disruption is hypothesized to stem from the difference in wild type strains utilized in our experiment. The parent strain used for this study, PO1f, and PO1d are listed in Table 2.2 with their respective phenotypes. In a previous studies, a PO1d strain of *Y. lipolytica* with a deletion of OCH1 was used for the wild type. OCH1 codes for a mannosyltransferase (Guerfal, et al., 2013). The absence of this enzyme results in the absence of N-glycan hypermannosylation (Guerfal, et al., 2013). This subsequently leads to higher homogenous glycoprotein production. If the PAH1 disruption does lead to greater protein concentrations, the extended lag phase observed in this paper could stem from protein-induced toxicity. Without the OCH1 deletion it is possible that PO1f results in the growth trajectory observed.

Table 2-2: *Yarrowia lipolytica* strains

Strain	Genotype/Description
Yarrowia lipolytica	
PO1d	MatA, leu2-270, ura3-302, xpr2-322
PO1f	MatA, leu2-270, ura3-302, xpr2-322, axp-2

2.3.3 Lipid droplet comparison

As the growth was not affected between the PO1f and the engineered strain, it was then of interest if the storage of lipids would be adversely affected. To detect whether there were differences, fluorescent imaging was performed on both strains. Bodipy fluorescent staining dye was utilized for this purpose.

Bodipy is generally utilized to fluoresce lipid droplets in cells. This however has not been tested with the physiological changes stemming from disrupted PAP. Most notably, in *S. cerevisiae* TAGs were still prevalent after the absence of PAH1 (Adeyo, et

al., 2011). If Bodipy localizes to the neutral lipids not associated with LDs, this could potentially skew results. To ensure that the LD fluorescing is constant regardless of physiology of the cell, a study was done with an enzyme localizing to LDs. ERG6, a gene that codes for a LD associated enzyme was utilized for this purpose. Both strains of interest were transformed with plasmids expressing an ERG6 gene hybridized with a DS Red fluorescent protein. These strains were grown in the appropriate nitrogen-limited selective media which induced LD formation while still retaining the plasmids in the cells.

The ERG6 DS Red complex and the Bodipy stain fluorescence were imaged at approximately 36 hours after inoculation into 25 mL flasks. FITC and TEX RED filters were utilized to visualize green and red fluorescence respectively. These images were then combined for an overlay with the bright light cell images to create fluorescing samples. The overlaid images revealed that localization of the Bopidy staining dye to coincide with the ERG6 DS Red complex. The ERG6 presented itself visually as a ring surrounding each respective LD while the Bodipy staining resulted in filled in areas

within these rings as in Figure 2-4. This showed that Bopidy would be useful for the lipid comparison with no issues with localization.

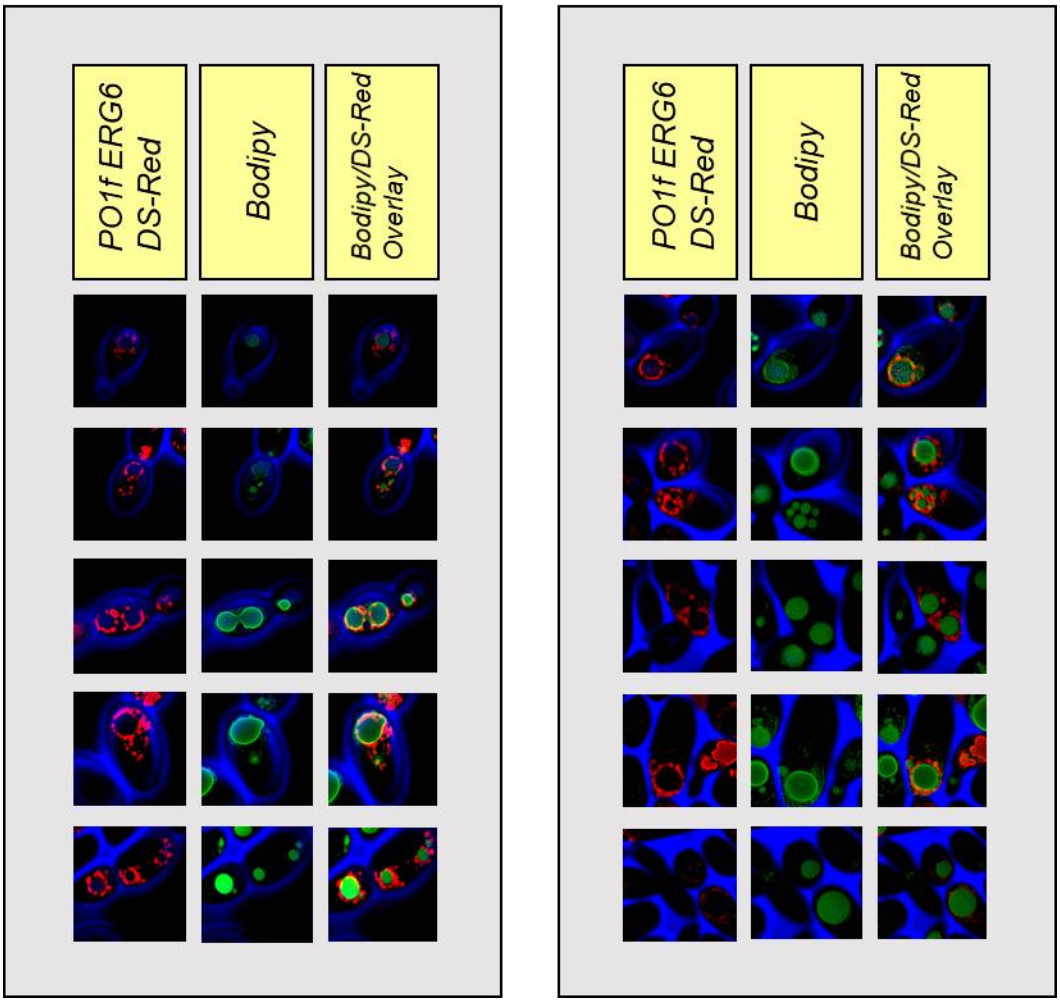

Figure 2-4: Fluorescent images of LDs in *Y. lipolytica*. Images were taken at 32 hours from nitrogen-limited media for optimal LD production. ERG6-DS Red localizes to the outside of the LDs while Bodipy stains the entirety of the LD. Overlay of images revealed that there is consistent localization of Bodipy to the LDs.

Strains that did not harbor the plasmid expressed ERG6 DS Red were grown in nitrogen-limited media for LD comparison. Cells were imaged at 24 hours with Bodipy

fluorescent stain as seen in Figure 2-5. Several images were taken to obtain roughly similar quantities of cell populations. Processed images were subjected to analysis in ImageJ software. All cell membranes were removed from the processed images and the LD field made monochromatic for analysis. LDs were automatically detected and separated based on the software while circularity parameters were implemented to remove erroneous. Circularity was based on a range from 0, representing a non-circular entity, to 1, a perfectly circular entity. For this study the circularity parameters of 0.25 to 1 proved effective for eliminating non-LD fluorescent marks. These parameters resulted in roughly 500 counts of LDs in *Δpah1* and over 1000 counts of LDs for PO1f. For both strains roughly 300 cells were tested. This suggested that LD quantity was reduced after gene disruption.

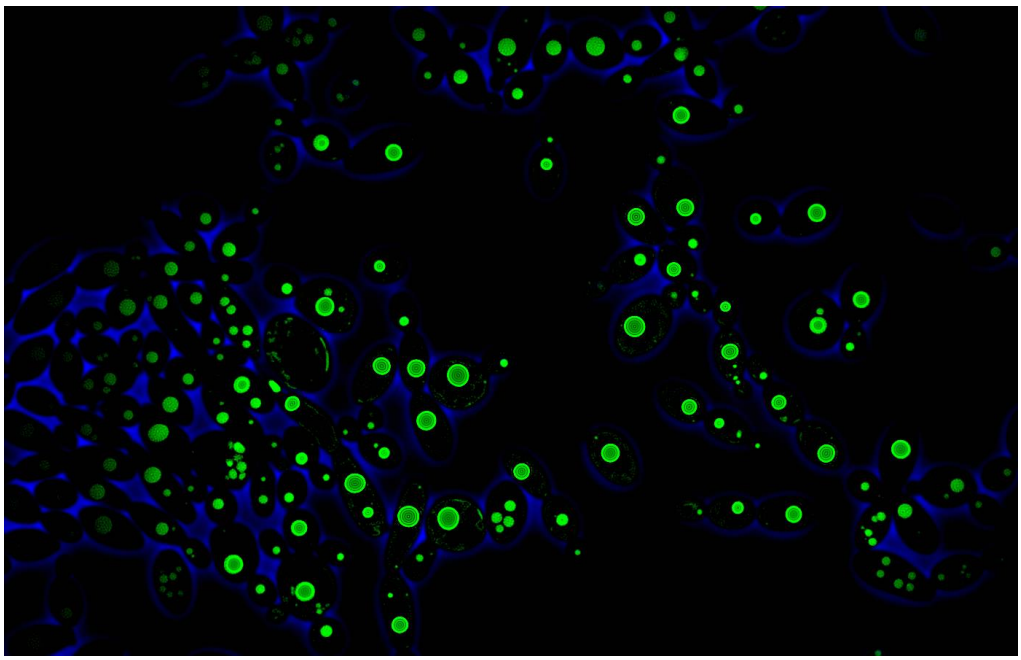

Figure 2-5: Sample cell field of Bodipy 493/503 staining. These cells were grown in nitrogen-limited media to induce LD formation. Cell membranes are shown in blue and LDs in green.

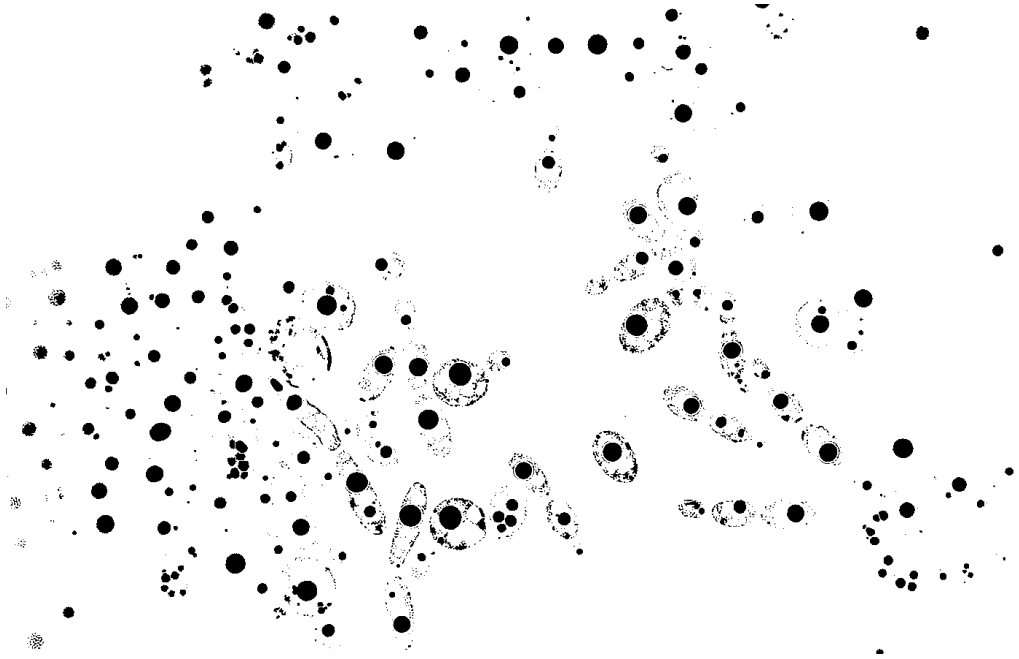

Figure 2-6: Sample LD field processed in ImageJ. The brightness threshold of the cell images were increased to over 150. Images were converted to black and white for better analysis

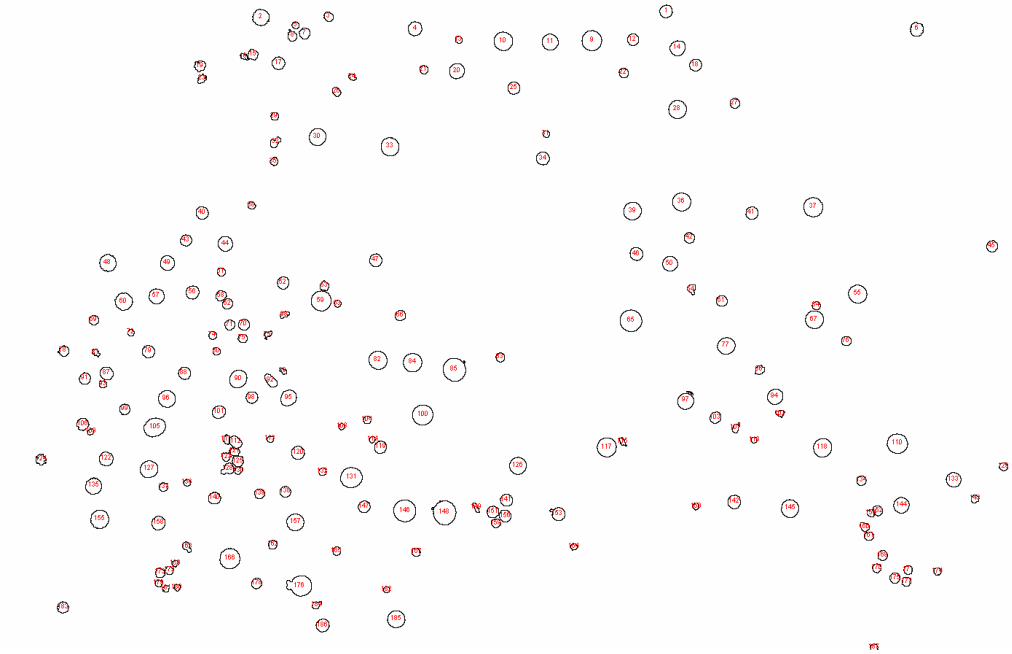

Figure 2-7: ImageJ LD recognition and counting. Black and white LD fields were analyzed in ImageJ software with a 25 square pixel minimum size exclusion parameter and a 0.25 circularity parameter.

The size of each LD was determined by ImageJ with the size listed as square pixels. The area was converted to square μm and the values plotted on a tree diagram shown in Figure 2-8. The median for the PO1f and *Δpah1* distributions were 84.28 μm^2 and 61.92 μm^2 respectively. The mean for the PO1f and *Δpah1* were 109.5 μm^2 and 78.23 μm^2 respectively. The total LD area dropped from 114944 μm^2 to 38098 μm^2 resulting in a 66% total LD reduction.

To ensure these values were distinctive, a one-sided t-test was performed on the LD sizes resulting in a P value less than 0.0001. The P value being lower than the P value corresponding to a 95% confidence interval confirmed that the decrease in LD size was statistically significant. The decrease in LD size between PO1f and *Δpah1* coincides with the hypothesis that PAP absence results in change in LD physiology. This LD size reduction is likely due to the carbon flux being diverted away from TAG formation. However, the continuing presence of the LDs suggest that either TAGs are still being formed or SEs are a large contributor to their size.

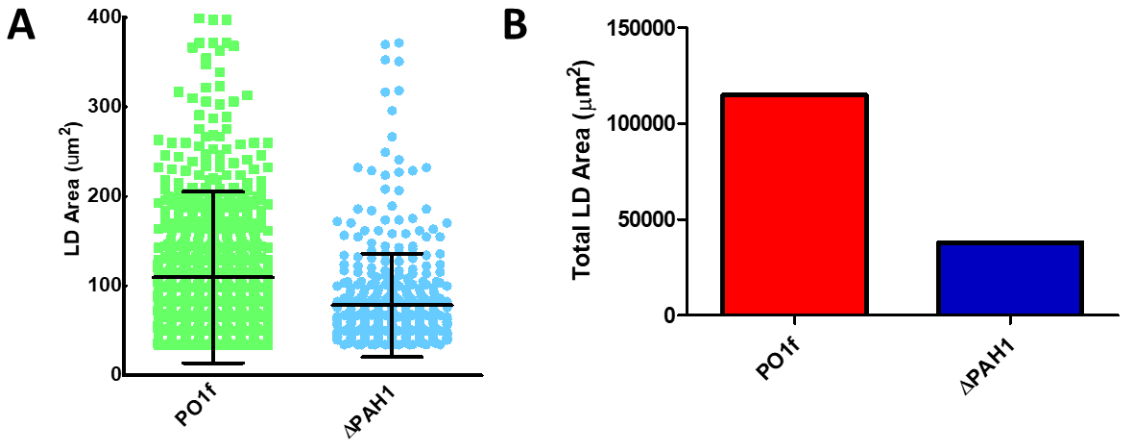

Figure 2-8: LD size distribution of PO1f and engineered strains. Cells were grown in nitrogen-limited media to stationary phase at 24 hours

2.3.4 ER Proliferation

The second change of cell physiology as a result of PAP deletion is believed to be ER proliferation. The proliferation has been stated to result in greater numbers of membrane stacks. To quantify this, ALK2-GFP fluorescence was measured using a plate reader. In addition to this, fluorescent imaging was done to determine any visual abnormalities.

Fluorescent imaging has the ability to elucidate any obvious changes in the ER. As the PAH1 disruption is believed to have a positive effect on the presence of the ER in *Y. lipolytica,* two main theories can be hypothesized. The first theory involves the increase in size of the ER relative to cell size. As ALK2-GFP localizes to the outer surface, this phenotype would result in larger perimeters of the ER. The second theory involves additional layers of ER stacks. In this scenario the outer perimeter determined by ALK2-GFP would not be discernibly different by visualization between PO1f and

engineered strains. However, there would be additional fluorescence due to membrane protein expression changes.

Fluorescent imaging was done with strains YS952 and YS953 to test ER changes visually. Both strains were grown to the same point in their respective growth phases. The results are shown in Figure 2-9. Images did not reveal any significant changes.

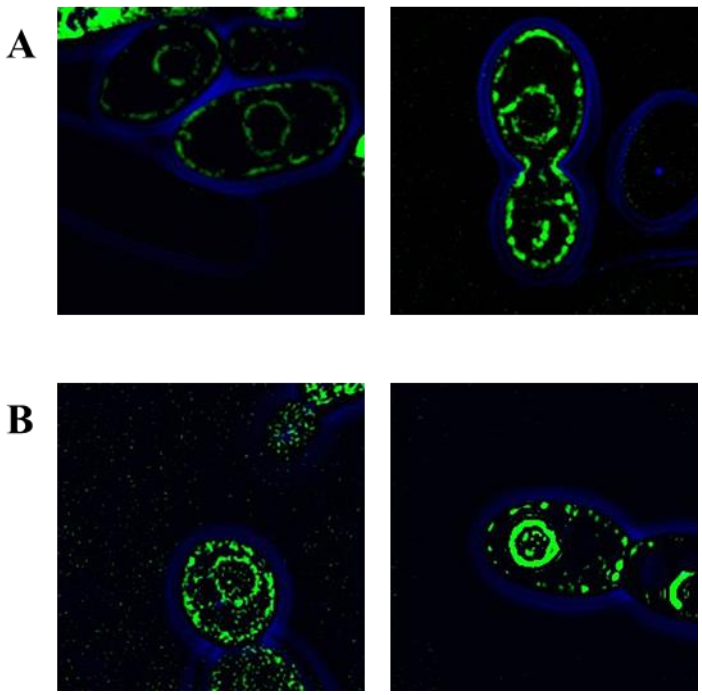

Figure 2-9: Fluorescent imaging of Alk2-GFP in PO1f and Δpah1. Images were taken of (A) PO1f background and (B) *Δpah1* background with a FITC filter set

Fluorescence measurements done with a plate reader contradicted this data. As shown in Figure 2-10 the expression seen in *Δpah1* was consistently higher in expression.

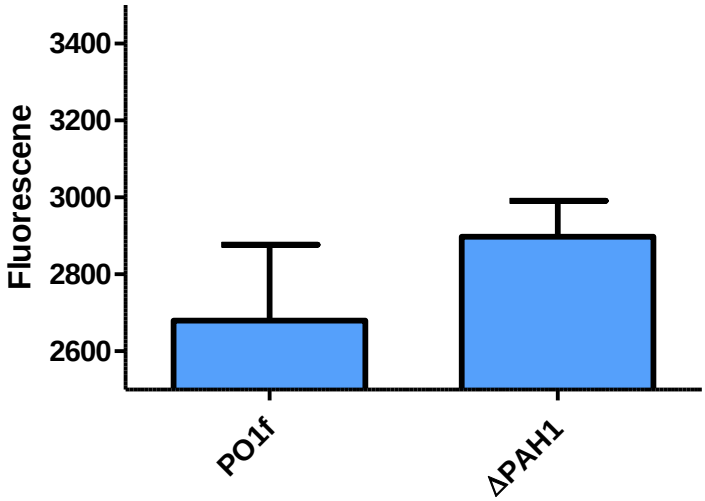

Figure 2-10: Plate reader fluorescence of yeast strains. Strains were transformed with ALK2-GFP and measured with an 485 nm excitation and 508 nm emission wavelength

PO1f background resulted in a median fluorescence value of 2449 while *Δpah1* had a higher median of 2783 which was a 13% increase. PO1f, however, had a higher deviation suggesting that differences to the PAH1 disruption could be statistically insignificant. It is of note though that the mean of the PO1f strains, 2679, was noticeably higher than the median suggesting that higher fluorescence values had impacted the result considerably. Furthermore, the 230 value difference compared to *Δpah1* roughly 100 value difference suggests that PO1f has impactful outliers. Overall the data suggests ALK2-GFP had bolstered expression after PAH1 disruption.

2.3.5 Discussion

The results in this study reveal the potential of altering cell physiology and quantifying said physiological change. The PAH1 gene was successfully disrupted utilizing genetic tools. The genomic disruption was confirmed via Sanger sequencing.

The protein sequence was also seen as having changes constituting inactivity or change substrate specificity of the pah1p.

Deletions of PAH1 in both *S. cerevisiae* and *Y. lipolytica* have resulted in growth deficiencies on specific substrates. For *Saccharomyces,* supplementation with palmitic acid was shown to be inhibitory to cell growth with an 8 hour increase in lag phase and 46% decrease in growth rate (Fakas, et al., 2011). Oleic acid supplementation to a concentration of 0.25 mM also resulted in an increased lag phase, albeit lower with a 5 hour extension (Fakas, et al., 2011). This fatty acid inhibition was seen in *Y. lipolytica* with growth in oleic acid media resulting in an 8 hour increase in lag phase (Guerfal, et al., 2013). The results of our study indicated no change in the growth characteristics after a PAH1 gene disruption in the PO1f strain of *Y. lipolytica.* This does not follow the expected trend of inhibition seen with both *Saccharomyces* and previous *lipolytica* experiments. This is expected to be a result of the genotype of the PO1f strain versus the strains utilized for other studies. For *Y. lipolytica*, it was shown that PO1d with an additional OCH1 deletion had inhibited uptake of oleic acid (Guerfal, et al., 2013). The PO1f strain utilized for this study did not have this OCH1 deletion in addition to having an AXP2 deletion as shown in table 2.2. This is believed to be the reason for the lack of growth deficiencies.

Previous studies of PAP in *S. cerevisiae* have elucidated that the phosphatase coded by PAH1, while not the only PAP, is the only one involved in lipid biosynthesis (Hardman, McFalls, & Fakas, 2017). In comparison, the homologues in *Y. lipolytica* have yet to be characterized. Activity studies on *Saccharomyces* have revealed that

phospholipid synthesis gene expression, nuclear and ER membrane growth, LD formation, and vacuole homeostasis and creation are affected by pah1p (Pascual & Carman, 2012). Mammalian cells have also been shown to harbor lipid degradation in the absence of PAP (Carman & Han, 2006). Our study wanted to determine if some of these physiological changes were observed in *Y. lipolytica* as well.

Physiological changes were determined with fluorescent microscopy experiments. In this study, PAH1 disruption lead to a decrease in LD size and number with a 66% and 50% reduction in total LD area and LD number respectively. In comparison to previous studies done on *S. cerevisiae* which observed 63% reduction in lipid droplet number (Adeyo, et al., 2011) our results are consistent. This reduction was likely due to carbon flux being diverted from TAG synthesis (Guerfal, et al., 2013). This is corroborated by deletions of PAH1 and steryl acyltransferase activity in *S. cerevisiae* that lead to an absence of LDs (Adeyo, et al., 2011). It should be noted however that this dual deletion still produced TAGs in comparable quantities to the wild type strain suggesting differences in PAP activity from *Y. lipolytica* to *S. cerevisiae.* LD composition and free fatty acid prevalence should be measured to further characterize the physiological change.

ER proliferation was measured with ALK2-GFP fluorescence which resulted in a 13% increase in protein expression from wild type to engineered strains. The increase in membrane protein expression has been observed within both *S. cerevisiae* and *Y. lipolytica* suggesting that the observed result in our study coincides with expected results.

To further emphasize this point fluorescent measurements of another membrane bound protein, likely Sec61p, should be done and compared.

The ER proliferation represents the second physiological change that stems from PAH1 disruption. With the ER proliferation it is now possible to test whether membrane protein expression can be increased to effectively characterize them and utilize them in industrial settings.

CHAPTER 3 : EXPLOITING PAH1 DISRUPTIONS FOR OVEREXPRESSION OF NATIVE ENZYMES

3.1 INTRODUCTION

The results of Chapter 2 of this thesis elucidated the changes that a disruption of PAH1 in *Y. lipolytica* has on the microorganism quantitatively. Most interestingly the ER was seen to have a slight potential proliferation with the addition of stacks of membrane from excess phosphatidic acid. This proliferation of the ER and subsequent effects that it could have on protein production are the subject of this chapter.

As discussed previously, P450s are a type of monooxygenase that are present in many organisms, including *Y. lipolytica* (Hirakawa, et al., 2009). One of their most prominent effects deals with their ability to functionalize different alkanes and substrates to be utilized by cells as sources of energy. The ALK series in *Y. lipolytica* is a prime example of this substrate utilization. Of the twelve enzymes that are included in this series the activities can be directed towards hydroxylating n-alkanes, the ω-terminal of long chain fatty acids, or both (Iwama, et al., 2016). External to cells, this hydroxylation has the ability to produce fatty acids and other oleochemicals that are industrially relevant.

In *lipolytica* the P450s that are associated with the ALK genes are membrane associated meaning they are bound to the ER (Iwama, et al., 2016). With this it can be hypothesized that changes in the proliferation of layers, degradation, or other alterations to the ER would have a substantial effect on the P450s in question (Guerfal, et al., 2013). As the PAH1 disruption in *lipolytica* has suggested ER proliferation within cells, it is of interest to see if the overproduction of P450s could be achieved. While native expression

has been previously shown to increase with the disruption of the PAP enzyme this chapter will investigate the expression of integrated overexpressions of the P450 associated the ALK2 gene.

3.2 METHODS AND MATERIALS

3.2.1 Strains, plasmids, and culturing

Strains used for this study are listed in Table 3-1.

Table 3-1: Yeast strains and plasmids used in Chapter 3 experiments

Strain	Genotype/Description	
Yarrowia lipolytica		
YS363	PO1f	
YS621	ΔPAH1	
YS863	ALK2-V5::PGA08	
YS864	ALK2-V5::PGA08, ΔPAH1	
YS894	ALK2-V5::PGA08, ALK2-V5::XPR2	
YS895	ALK2-V5::PGA08, ALK2-V5::XPR2, ΔPAH1	
YS926	ALK2-V5::PGA08, ALK2-V5::XPR2, ALK2-V5::PGD17	
YS927	ALK2-V5::PGA08, ALK2-V5::XPR2, ALK2-V5::PGD17, ΔPAH1	
Strain	**Genotype/Description**	**Marker**
Yarrowia lipolytica		
YS952	YS363 + pIW225	Amp/LEU
YS953	YS621 + pIW225	Amp/LEU
YS984	YS863 + pIW225	Amp/LEU
YS985	YS864 + pIW225	Amp/LEU
YS986	YS894 + pIW225	Amp/LEU
YS987	YS895 + pIW225	Amp/LEU
YS988	YS926 + pIW225	Amp/LEU
YS989	YS927 + pIW225	Amp/LEU
Plasmids	**Genotype/Description**	
pIW 225	TEF-ALK2-GFP-CYC1	Amp/LEU

3.2.2 ALK2 Genomic Integrations

Integrations of Alk2-V5 were achieved with a dual plasmid system utilizing CRISPR/Cas9. The CRISPR/Cas9 system was designed for each insertion site to target and induce a double-stranded break in the gene of interest. A second plasmid designed with 1kb flanking regions surrounding the respective insertion site utilized.

The plasmids has two markers for selection. AmpR allows the plasmid to be amplified in competent *E. Coli* cells after proper cloning. Leu2 and Ura3 promote growth of transformed strains on minimal media.

The CRISPR/Cas9 plasmid included a 20 base pair PAM sequence, a sequence preceding a NGG segment, that was followed by sgRNA which targeted the PAM sequence in the genome. The Cas9 protein then induced a double stranded break in the genomic DNA.

Repairs in the genome were done with either homologous recombination (HR) or non-homologous end joining (NHEJ). The secondary plasmid HR plasmid used 1kb regions that correspond to areas upstream and downstream of the induced genomic double stranded break to incite homologous recombination. Three sites were utilized for genomic integrations – XPR2, PGA08, and PGD17 – with each having separate sets of plasmids for integration. The HR plasmid was designed with the ALK2-V5 cassette within the flanking regions for potential insertion. The V5 sequence was designed using codon optimization and was introduced to the ALK2-associated P450 with a glycine-serine linker.

Strains were tested for integration by first performing colony PCR for correct length amplifications. The region of insertion was then amplified and sent for Sanger sequencing with positive samples being grown in YPD to induce selective pressure removal of the plasmids.

3.2.3 ALK2-GFP plasmid transformations

Single plasmid transformation was performed with a Frozen-EZ Yeast Transformation kit purchased from Zymo Research. This kit utilized a lithium acetate based transformation protocol. Yeast strains were grown overnight and then inoculated in a 1:10 ratio in the appropriate rich or minimal media. After the strains reached exponential phase, 4-6 hours after inoculation, the cells were pelleted and resuspended in EZ1 solution. Cells were again pelleted and suspended in EZ2 solution. Approximately 1 μg of DNA was introduced to 50 μL of the competent cells. An additional 500 μL of EZ3 was added to the competent cells and the solution incubated for 45 minutes. The cells were also vortexed every 15 minutes of the inoculation. Samples were either plated or inoculated in liquid media for 2-4 days. Strains with fluorescent markers were imaged to ensure proper transformation.

3.2.4 qPCR

Yeast strains were grown overnight in the appropriate culturing media. 1 mL of each respective culture was pelleted. Each pellet was subjected to RNA extraction with a YeaStar RNA isolation kit from Zymo Fisher. To decompose any residual DNA, 40 μL of each RNA sample was combined with 5 μL of DNase I and 5 μL of DNA digestion

buffer. This solution was incubated at room temperature for 15 minutes. The resulting RNA mixture was then subjected to RNA purification with a kit from Zymo Fisher.

Reverse transcription was performed with a iScript Reverse Transcription Supermix from BioRad. The resulting cDNA was diluted in a 1:10 ratio in nuclease free water. Approximately 2 µL of the diluted cDNA solution was utilized with Universal SYBR Green Supermix for qPCR.

3.2.5 SDS-PAGE

Yeast strains were grown overnight and normalized to the same OD. 750 µL of each yeast sample was pelleted and the supernatant removed. Cell lysis was achieved with 200 µL of 0.1M NaOH added to the pelleted for 10 minutes at room temperature. Solutions were then centrifuged for two minutes at 8000 RPM and the supernatant discarded. The lysed cell pellet was then suspended in 100 µL 2X sample buffer and boiled at 98^0C for 10 minutes. Samples were centrifuged at 10,000 RPM for 1 min and loaded into wells of the PAGE gel. Samples were subjected to electrophoresis in SDS loading buffer for 1 hour at 150 volts. A ChemiDoc Imager from BioRad was utilized for identifying the total protein concentration for each lane. The images were taken in ImageLab software. The Stain Free Gel-Protein Gels application was used with automatic detection of intense bands.

3.2.6 Western blot analysis

Samples loaded on SDS-PAGE gels were transferred to Western blotting membranes in transformation buffer overnight at 25 volts. The membrane was washed three times with 30 mL TBST for 10 minute intervals. Blocking was performed with 5%

nonfat milk in TBST for one hour. Hybridization was done for one hour with an anti-V5 antibody from Sigma Aldrich. The membrane was again washed for with TBST four times at seven minutes each. A second hybridization was done with a goat anti-rabbit IgG antibody for 30 minutes. The second washing step was repeated and an HRP substrate added. A ChemiDoc Imager was utilized for identifying the Western blot chemiluminescence stain. The images were taken in ImageLab software. The Chemi Hi Sensitivity application was used with automatic detection of intense bands.

3.2.7 Flow Cytometry

Strain samples were grown in triplicate to stationary phase and normalized based on OD. Each sample was diluted to an OD between 0.1 and 1.0. Each sample was subjected to flow cytometry where 10,000 events were counted. The resulting distributions were gated in FlowJo software to ensure that healthy cells with desirable morphology would be compared.

3.2.8 Plate Reader Fluorescence

Strain samples were grown in triplicate to stationary phase and normalized based on OD. Cell were then washed twice with water and suspended in 200 μL of water. Samples were loaded into a black CorningStar 96-well plate and fluorescence measured with a 485nm excitation and 508nm emission filter. The sensitivity setting was set to 100 due to promoter strength.

3.2.9 Fluorescent Imaging

Imaging was done with an Olympus BX51 fluorescent microscope at the time point specified for the experiment. Samples were washed twice in PBS before beginning

prepared on glass slides for visualization. Bright light images were taken for the full images of the cell membrane and other organelles discernible without stains. Strains transformed with DS Red fluorescing plasmids were imaged with a Texas Red filter set. Samples stained with Bodipy 493/503 were imaged with a FITC filter set. All images were recorded with a QImaging Retiga Exi Fast 1394 camera in cellSens Dimension software. Images were processed via deconvolution and all bright fields were combined with respective fluorescent views.

3.3 RESULTS AND DISCUSSION

3.3.1 Genomic Integrations

ALK2-V5 complexes were integrated into the genome of PO1f and *Δpah1*. The ALK2 was chosen as it has been studied previously. The V5 tag was an addition for the chemiluminescent quantification of protein expression. Each background had single, double, and triple integrations into the genome into PGA08, XPR2, and PGD17 sites in order respectively.

To achieve integrations a dual plasmid transformation was used. For each insertion site a CRISPR/Cas9 plasmid targeted the site an induced a double stranded break. The second plasmid used homologous regions to insert an ALK2-V5 sequence. To test for integrations a three primer gene amplification system as shown in Figure 3.1 was utilized. Primer 1 and 2 flanked the respective insertion site while primer 3 annealed at the terminator of the ALK2-V5 sequence. This system resulted in one of three results that were visible with gel electrophoresis: a 2 kb band for a homogeneous colony without an ALK2-V5 integration, a 1 kb band for a homogeneous colony with an ALK2-V5

integration, and both bands for a heterogeneous colony with and without integrations. Figure 3.2 shows an example of the different gel electrophoresis outcomes from the primer system.

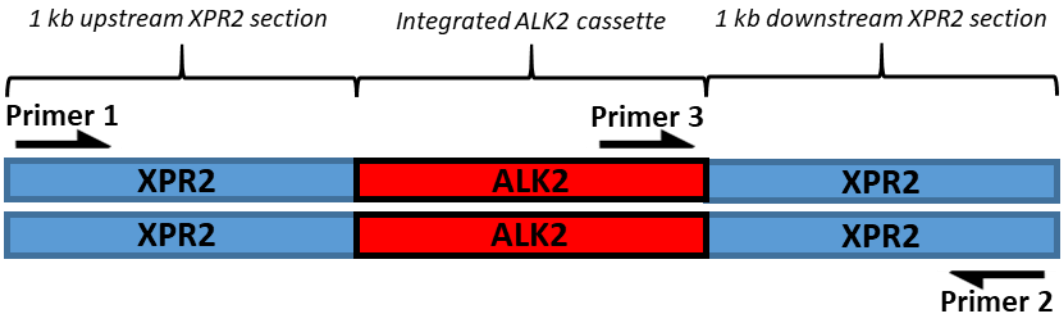

Figure 3-1: Three primer amplification system for determination of ALK2-V5 integrations into *Y. lipolytica* genome. Primers flank homology regions.

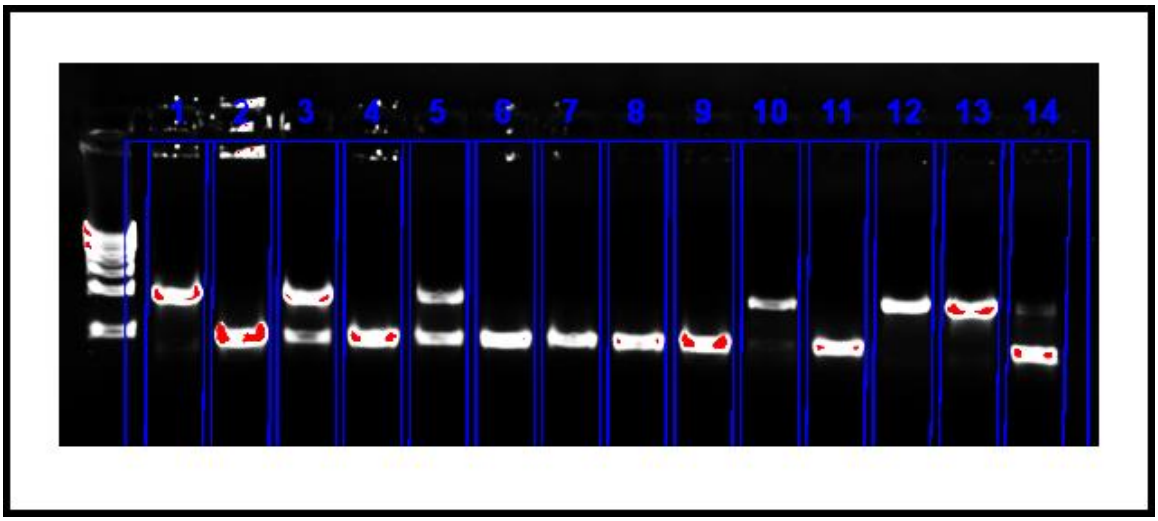

Figure 3-2: Gel electrophoresis of amplified genomic fragments from the three primer system. The sample used a 1 kb ladder with three possible results in each sample lane: 1 kb, 2 kb, and both bands.

For each of the integration sites the integration frequency, as shown in table 3.2, was determined based on the relative number colonies tested for integrations versus the total number of cells that were successfully transformed and tested.

Table 3-2: Integration efficiency of ALK2-V5 cascade into subsequent sites.

Integration Order	Integration Site Tested	Number of Samples	Homogeneous Colonies	Heterogeneous Colonies	Integration Efficiency
1st	PGA08	10	5	5	100%
2nd	XPR2	14	1	9	71%
3rd	PGD17	12	1	3	25%

For each subsequent integration of ALK2-V5 into *Y. lipolytica* there was an overall decrease in the integration efficiency. The frequency included all samples that either suggested a homogeneous colony with an integration or a heterogeneous colony with cells that contain integrations. The decrease in integration efficiency suggests that there is difficulty in expressing multiple copies of the ALK2 associated P450.

3.3.2 Protein overexpression

The first step in determining the usefulness of PAH1 disruptions to overexpress key membrane associated enzymes like P450s is to show the change in protein expression of integrated P450s. For this study the target protein is the ALK2 associated P450. Alk2p has activity towards alkanes with a 16 length carbon backbone such as hexadecane. It was selected due previous experiments tailored to measuring the activity of P450s.

Strains integrated with one, two, or three copies of an ALK2-V5 complex in inactive sites (AXP, XPR2, and PGD17) were utilized for comparison of the PAH1 disruption to a PO1f background. After each strain was grown and normalized to similar ODs, each sample was then lysed. These lysates were used for SDS-PAGE to separate all proteins based on size exclusion. The gels were then imaged to ascertain the total protein amount in each sample as seen in Figure 3-3.

The total protein concentration was useful in normalizing the Western blot data obtained after blocking. With comparing the relative protein amount in each concentration, changes in expression could be normalized to avoid slight errors in protein concentration.

Western blot analysis was performed on the respective samples from the SDS-PAGE experiment. Each lane was normalized based on the original gel resulting in modified intensity values. The membranes for the Westerns showed a gradual increase in expression for each subsequent ALK2-V5 integration in both PO1f and *Δpah1* backgrounds as shown in Figure 3-3.

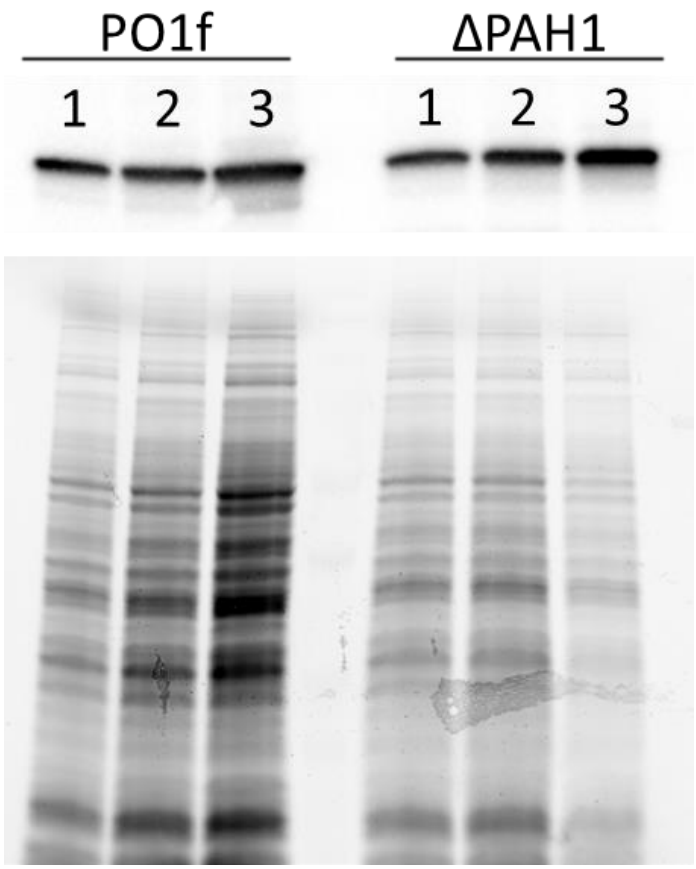

Figure 3-3: Western blot analysis and SDS-PAGE of *Y. lipolytica* samples. Each additional ALK2-V5 integration is represented by designation 1, 2, or 3. Each lane is a corresponding SDS sample and Western signal.

Each Western blot normalized intensity value was again normalized relative to the expression of ALK2-V5::PGA08 (YS863) in the respective experiment These values were averaged and plotted in comparison to each other as shown in Figure 3-4. The findings in the graph corroborated the results seen in the Western blot images. Most notably the triple integrations in the *Δpah1* background maintained significantly higher protein expression than that of the PO1f background and single/double Δpah1 background strains. YS 927 did have greater variation than the other tested strains;

however, the lower end of the error range was still considerably higher than any other strain tested.

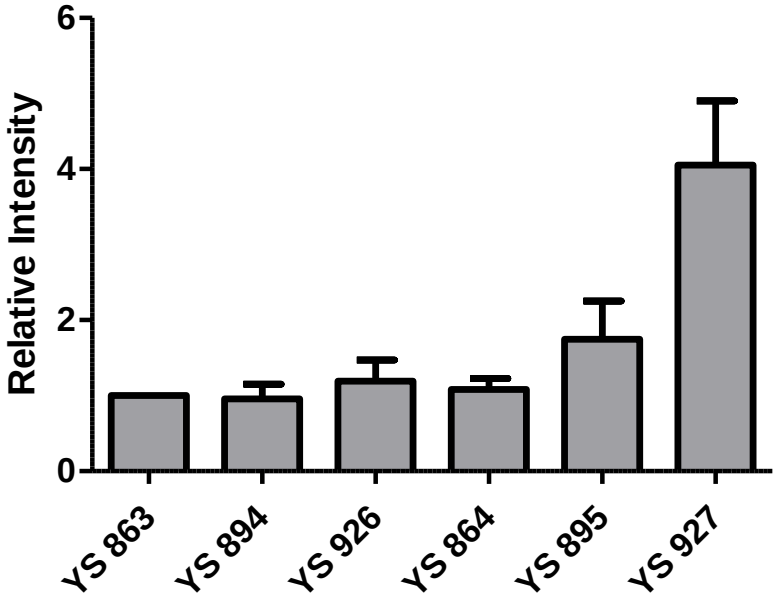

Figure 3-4: Western intensity comparisons. Western samples were normalized to PO1f with a single ALK2-V5 integration.

3.3.3 Gene expression

Relative gene expression of ALK2 was determined using qPCR. Measuring the change in gene expression elucidates the cellular response to the overexpression of ALK2 within the genome. The fold change was determined relative to YS 863 which has a PO1f background and one genomic integration of ALK2-V5. The average fold change values were graphed in comparison to one another in Figure 3-5.

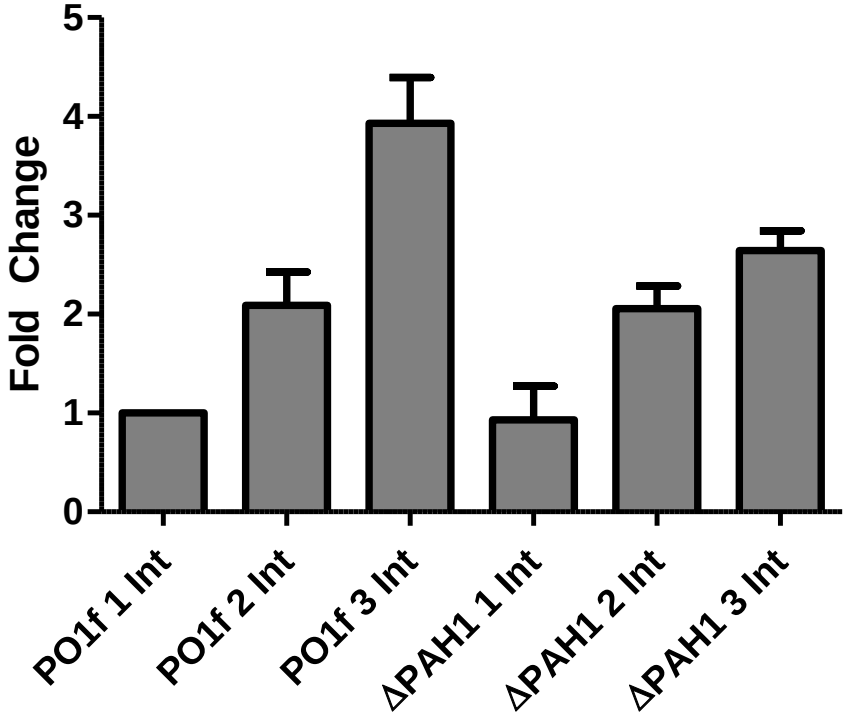

Figure 3-5: Average qPCR copy number fold change of each strain relative to PO1f background. Samples were grown to mid-stationary phase in rich media.

The PO1f background strains maintained higher expression levels than their PAH1 disruption counterparts. Graphing translational data versus transcription data for each of these strains shows higher protein expression response in relation to gene expression for PAH1 disrupted strains versus PO1f strains as shown in Figure 3-6. This relationship could be the result of several factors. Protein degradation in response to limits in the ER could be a main culprit. The capacity of the ER could limit the P450s associated with it which would result in the lower PO1f expression that was seen in the Western blot data. To determine if the capacity of the ER is limiting to P450 production excess P450s were expressed.

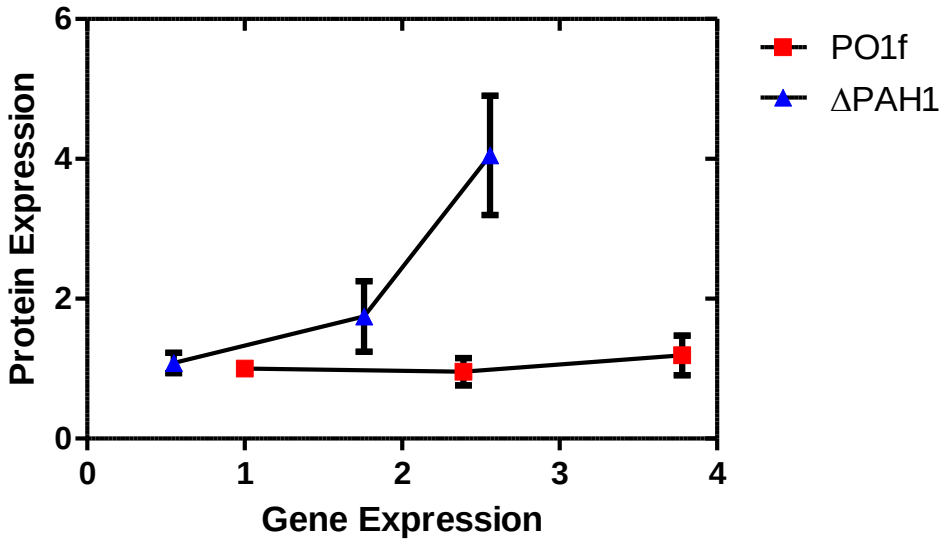

Figure 3-6: Comparison of relative gene expression versus protein expression for ALK2 genes

3.3.4 ER capacity measurements

As the ALK2-GFP plate reader data from Chapter 2 and the Western blot data previously in this chapter suggest, there is proliferation of the ER. The Western analysis also provided evidence that the proliferation can be beneficial for membrane protein production; however, the increase of the ER with regards to additional proteins has yet to be tested. The capacity has the ability to elucidate the limitations in overexpressions of P450s and other enzymes in these strains. Determining capacity also has the benefit of revealing how much additional protein can be overexpressed, whether Alk2p or otherwise.

For this study the capacity was measured predominantly using ALK2-GFP fluorescence measurements and imaging. Imaging was done during the stationary phase for overexpression strains transformed with a plasmid expressing ALK2-GFP (pIW225). The results of the fluorescent imaging are shown in Figure 3-7.

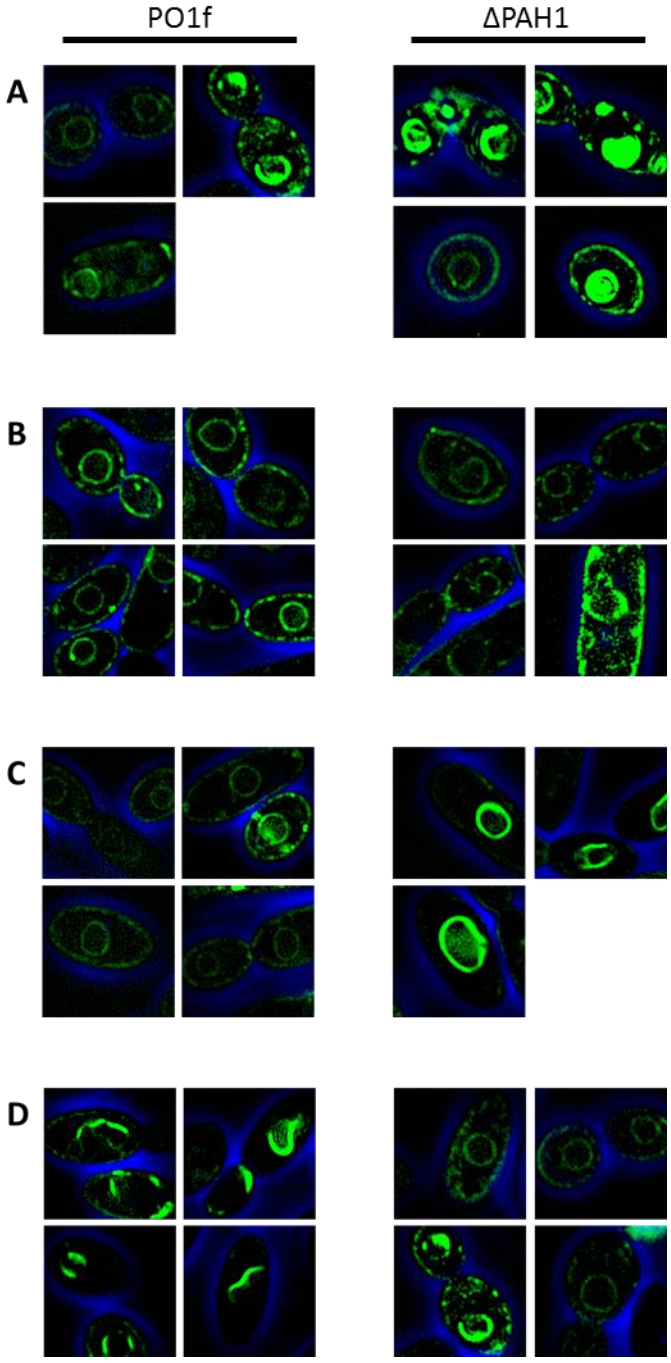

Figure 3-7: Fluorescent imaging of stains transformed with ALK2-GFP. Each set of images represent the following number of integrations of ALK2-V5: (A) 0, (B) 1, (C) 2, and (D) 3.

The imaging for the first two integrations in both backgrounds results in similar ER structures. However, the third integration into a PO1f background strain shows differences in expression. Unlike the PAH1 disruption counterparts, the ER does not fluoresce around the entire perimeter. As the expression in single and double integrations remains similar this could suggest that the ER capacity is limiting further expression beyond three genomic expressions. This idea is further corroborated by the ER in YS 989 having its perimeter completely fluoresce meaning that increased capacity allows it to hold the additional P450s.

3.3.5 Discussion

The P450 membrane protein expression was observed increasing after the disruption of PAP. This coincides with the increase of expression of other natively expressed membrane proteins from other sources including Bap31, B-cell associated receptor, and NS4, non-structural protein (Guerfal, et al., 2013). This was consistent among each subsequent genomic integration of the ALK2-associated P450. Western analysis showed that the overexpressed protein constituted higher percentages of the total system proteins. Overall the best performer was YS927 which achieved a 4 fold increase in expression of the V5 marker compared to that of the YS863. More importantly the PAH1 disruption added greater expression than their PO1f counterparts. This suggests the PAH1 disruption does incite more Alk2p expression. However, the Western blot analysis alone does not reveal if these expression increases are uninhibited by other cellular functions.

Though protein expression had increased, gene expression had been shown to decrease after the PAH1 disruption as revealed with the qPCR data. Figure 3-6 showed that protein expression with respect to gene expression increased faster in PAH1 disrupted backgrounds than in PO1f backgrounds. If no external factors were involved in the transcription and translation processes then the change in expression should have been no difference in protein versus gene expression from wild type to disrupted strains. This showed that the increased protein presence observed in the Westerns was not a result of increased transcription. Instead there is likely either protein degradation that occurs in the PO1f strain or regulation of protein translation that takes place. ER associated degradation (ERAD) is a likely culprit. In *Saccharomyces cerevisiae* proteins that are misfolded in different domains are subjected to ERAD (Chantret, Kodali, Lahmouich, Harvey, & Moore, 2011). It is likely that a homologous response in *Y. lipolytica* degrades proteins in excess of the ER capacity. Another possibility is the induction of the transcription of phospholipid biosynthesis enzymes. It has been hypothesized that increased levels of chaperones causes a cellular response that generates more ER membrane to accommodate additional protein in *S. cerevisiae* (Santos-Rosa, Leung, Grimsey, Peak-Chew, & Siniossoglou, 2005). This suggests that increasing protein prevalence as a result of PAP disruption not only causes an initial increase in membranes due to increased flux through the phospholipid biosynthesis pathway, but the increased protein concentration induces a secondary membrane proliferation due to the increased need of chaperones for the system.

Fluorescent imaging supported the claim that protein degradation affected the ability of P450s to be expressed in PO1f. Multiple integrated copies of the ALK2 gene coupled with the transformation of the fluorescent protein ALK2-GFP revealed ALK2-GFP localization was limited to part of the ER for PO1f as opposed to the entirety of the ER for *Δpah1*. This protein limitation suggests that the ER has capacity limits that can be reached with engineered expression. It can also be seen that proliferating the ER has the effect of increasing the capacity of the ER to hold additional proteins.

CHAPTER 4 **CHAPTER 4: CONCLUSION & RECOMMENDATIONS**

P450s are industrially desirable proteins that can be used for the creation of a variety of oleochemicals and useful sustainable products. In this study, the goal was to ascertain the potential overexpression of P450s with particular genetic changes. The disruption of PAH1 proved to be an effective method of increasing manufactured changes in expressions.

The study began with elucidating effects of a PAH1 disruption within *Y. lipolytica*. This was done by measuring the changes in lipid droplet morphology after genetic manipulation. Fluorescent imaging analysis revealed a significant size reduction in LDs after gene disruption with a certain level of LDs being conserved due to their inclusion of sterol esters and TAGs produced outside the traditional Kennedy pathway. ER proliferation was determined to change after rendering PAP inactive by utilizing fluorescence of membrane proteins. PO1f was expected to undergo more proliferation of ER resulting in more stacks after PAH1 disruption. This phenotype was observed with the increased fluorescence of ALK2-GFP.

From this we decided to study and utilize disruptions in PAH1 in relation to membrane bound proteins, in particular P450s. Through genetic integrations we were able to generate strains that harbored overexpressed native enzymes. Western blot analysis showed the protein expression associated these genetic alterations. There was an additional increase in expression in PAH1 disrupted strains stemming from proliferated ER. Quantitative PCR revealed a decrease in gene expression after disrupting PAH1.

With fluorescent imaging it was then proposed that the ER is limited in capacity which can be rectified with PAH1 disruptions.

These experiments provide a starting point in discovering the ability of *Y. lipolytica* in producing P450s in industrially relevant quantities. It is shown that P450s can be increased in expression through physiological changes in cells. Furthermore, it provides some genetic methods to further potential membrane protein generation. Moving forward the likelihood of having overexpressed P450s being correctly folded should be researched. This would involve discovering the relative activity of samples using either substrate titration or a carbon monoxide assay. If proteins exist in high enough quantities, then expressing different native proteins could be done to help characterize a variety of enzymes or design systems for excreting the commercially lucrative ones. Furthermore, the ER capacity should be further tested by determining if the variable protein expression of ALK2-GFP is due to preferred expression spurred by competition between genomic ALK2 and vector ALK2.

CHAPTER 5 References

Adeyo, O., Horn, P. J., Lee, S., Binns, D. D., Chanadrahas, A., Chapman, K. D., & Goodman, J. M. (2011). The yeast lipin orthologue Pah1p is important for biogenesis of lipid droplets. *The Journal of Cell Biology*, 1043-1055.

Arendt, P., Miettinen, K., Pollier, J., Rycke, R. D., Callewaert, N., & Goossens, A. (2017). An endoplasmid reticulum-engineered yeast platform for overproduction of triterpenoids. *Metabolic Engineering*, 165-175.

Beopoulos, A., Mrozova, Z., Thevenieau, F., Le Dall, M.-T., Hapala, I., Papanikolaou, S., . . . Nicaud, J.-M. (2008). Control of Lipid Accumulation in the Yeast *Yarrowia lipolytica*. *Applied and Environmental Microbiology*, 7779-7789.

Blazeck, J., Hill, A., Liu, L., Knight, R., Miller, J., Pan, A., . . . Alper, H. (2013). Harnessing *Yarrowia lipolytica* lipogenesis to create a platform for lipid and biofuel production. *Nature Communications*.

Bordeaux, M., Galarneau, A., & Drone, J. (2012). Catalytica, Mild, and Selective Oxyfunctionalization of Linear Alkanes: Current Challenges. *Angewandte Minireviews*, 10712-10723.

Carman, G. M., & Han, G.-S. (2006). Roles of phosphatidate phosphatase enzymes in lipid metabolism. *Biochemical Sciences*.

Carman, G. M., & Han, G.-S. (2009). Regulation of phospholipid synthesis in yeast. *Journal of Lipid Research*.

Carman, G., & Han, G.-S. (2009). Phosphatidic Acid Phosphatase a Key Enzyme in the Regulation of Lipid Synthesis. *Journal of Biological Chemistry*.

Chantret, I., Kodali, V., Lahmouich, C., Harvey, D. J., & Moore, S. E. (2011). Endoplasmic Reticulum-associated Degradation (ERAD) and Free Oligosaccharide Generation in *Saccharomyces cerevisiae*. *Journal of Biological Chemistry*, 41786-41800.

Fakas, S., Qiu, Y., Dixon, J. L., Han, G.-S., Ruggles, K. V., Garbarino, J., . . . Carman, G. M. (2011). Phosphatidate Phosphatase Activity Plays Key Role in Protection against Fatty Acid-induced Toxicity in Yeast. *The Journal of Biological Chemistry*, 29074-29085.

Fasan, R. (2012). Tuning P450 Enzymes as Oxidation Catalysts. *ACS Catalysis*, 647-666.

Fickers, P., Benetti, P.-H., Wache, Y., Marty, A., Mauersberger, S., Smit, M., & Nicaud, J.-M. (2005). Hydrophobic substrate utilisation by the yeast *Yarrowia lipolytica*, and its potential applications. *FEMS Yeast Research*, 527-543.

Friedlander, J., Tsakraklides, V. K., Greenhagen, E. H., Consiglio, A. L., MacEwen, K., Crabtree, D. V., . . . Stephanopoulos, G. (2016). Engineering of a high lipid producing *Yarrowia lipolytica* strain. *Biotechnology for Biofuels*.

Gao, M., Cao, M., Suastegui, M., Walker, J., Quiroz, N. R., Wu, Y., . . . Shao, Z. (2016). Innovating a Nonconventional Yeast Platform for Producing Shikimate as the Building Block of High-Value Aromatics. *ACS Synthetic Biology*.

Guerfal, M., Claes, K., Knittelfelder, O., Rycke, R. D., Kohlwein, S. D., & Callewaert, N. (2013). Enhanced membrane protein expression by engineering increased intracellular membrane production. *Microbial Cell Factories*.

Han, G.-S., O'Hara, L., Carman, G., & Siniossoglou, S. (2008). An unconventional diacylglycerol kinase that regulates phospholipid synthesis and nuclear membrane growth. *Journal of Biological Chemistry*.

Hardman, D., McFalls, D., & Fakas, S. (2017). Characterization of phosphatidic acid phosphatase activity in the oleaginous yeast *Yarrowia lipolytica* and its role in lipid biosynthesis. *Yeast*, 83-91.

Hirakawa, K., Kobayashi, S., Inoue, T., Endoh-Yamagami, S., Fukuda, R., & Ohta, A. (2009). Yas3p, an Opi1 Family Transcription Factor, Regulates Cytochrome P450 Expression in Response to n-Alkanes in *Yarrowia lipolytica*. *Journal of Biological Chemistry*.

Iwama, R., Kobayashi, S., Ishimaru, C., Ohta, A., Horiuchi, H., & Fukuda, R. (2016). Functional roles and substrate specificities of twelve cytochromes P450 belonging to CYP52 family in n-alkane assimilating yeast *Yarrowia lipolytica*. *Fungal Genetics and Biology*, 43-54.

Kaspera, R., & Croteau, R. (2006). Cytochrome P450 oxygenases of Taxol biosynthesis. *Phytochemistry Reviews*, 433-444.

Li, H., & Alper, H. S. (2016). Enabling xylose utilization in *Yarrowia lipolytica* for lipid production. *Biotechnology Journal*.

Muller, S., Sandal, T., Kamp-Hansen, P., & Dalboge, H. (1998). Comparison of Expression Systems in the Yeasts *Saccharomyces cerevisiae, Hansenula polymorpha, Klyveromyces lactis, Schizosaccharomyces pombe* and *Yarrowia lipolytica*. Cloning of Two Novel Promoters from *Yarrowia lipolytica*. *Yeast*, 1267-1283.

Nebert, D., & Russell, D. (2002). Clinical importance of the cytochromes P450. *The Lancet*, 1155-1162.

Notonier, S., Gricman, L., Pleiss, J., & Hauer, B. (2016). Semi-rational protein engineering of CYP153AM.aq.-CPRBM3 for efficient terminal hydroxylation of short to long chain fatty acids. *ChemBioChem*, 1550-1557.

Pascual, F., & Carman, G. M. (2012). Phosphatidate phosphatase, a key regulator of lipid homeostasis. *Biochimica et Biophysica Acta (BBA) - Molecular and Cell Biology of Lipids*, 514-522.

Qiao, K., Wasylenko, T. M., Zhou, K., Xu, P., & Stephanopoulos, G. (2017). Lipid production in *Yarrowia lipolytica* is maximized by engineering cytosolic redox metabolism. *Nature Biotechnology*.

Santos-Rosa, H., Leung, J., Grimsey, N., Peak-Chew, S., & Siniossoglou, S. (2005). The yeast lipin Smp2 couples phospholipid biosynthesis to nuclear membrane growth. *The EMBO Journal*, 1931-1941.

Scheller, U., Zimmer, T., Becher, D., Schauer, F., & Schunck, W.-H. (1998). Oxygenation Cascade in Conversion of n-Alkanes to a,o-Dioic Acids Catalyzed by Cytochrome P450 52A3. *The Journal of Biological Chemistry*, 32528-32534.

Sheng, J., & Feng, X. (2015). Metabolic engineering of yeast to produce fatty acid-derived biofuels: bottlenecks and solutions. *Frontiers in Microbiology*.

Shimada, T., & Fujii-Kuriyama, Y. (2003). Metabolic activation of polycylic aromatic hydrocarbons to carcinogens by cytochromes P450 1A1 and 1B1. *Cancer Science*.

Souza, K. S., Ramos, C. L., Schwan, R. F., & Dias, D. R. (2016). Lipid production by yeasts grown on crude glycerol from biodiesel industry. *Preparative Biochemistry and Biotechnology*.

Xu, Z., Su, W.-M., & Carman, G. (2012). Fluorescence spectroscopy measures yeast PAH1-encoded phosphatidate phosphatase interaction with liposome membranes. *Journal of Lipid Research*.